Oringins of GeV- TeV scale Cosmic-Ray Physics

(Dark Matter vs Pulsar/SNR)

Yong-Yeon Keum
IBS, Seoul National University

CosPA 2015
12-16 October, 2015
KAIST Munji Campus, Daejeon in Korea

Contents :

- Motivations

- PAMELA-CREAM Anomaly
- Understanding of power-law behavior
- Green Function Method
- Resolve the CREAM-PAMELA Anomaly : A&A 555 A48 (2013)

- Production of Antimatters in the Galaxy :
  PAMELA and New AMS02 data (positron and antiproton flux)
- Some Hopes (Dark-Matter vs Pulsar Scenarios)

- Results and Discussions

Motivations:

Why GeV-TeV scale Cosmic Ray Physics are so interesting and important ?

-- Recently many observation data came out: CREAM, PAMELA, FERMI, HESS, AMS02, ...

-- Hopes to understand the property of Dark-Matter, Anti-Matter, Diffusion and Transport Mechanism of CR.

Introduction-01

DM exists

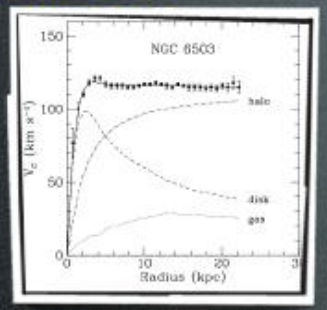

galactic rotation curves

weak lensing (e.g. in clusters)

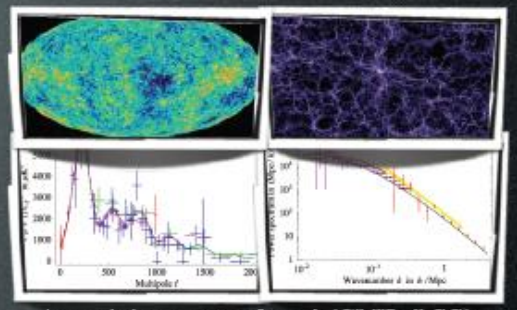

'precision cosmology' (CMB, LSS)

DM is a neutral, very long lived, weakly interacting particle.

Some of us believe in the WIMP miracle.

- *weak*-scale mass (10 GeV - 1 TeV)
- *weak* interactions $\sigma v = 3 \cdot 10^{-26} \mathrm{cm}^3/\mathrm{sec}$
- give automatically correct abundance

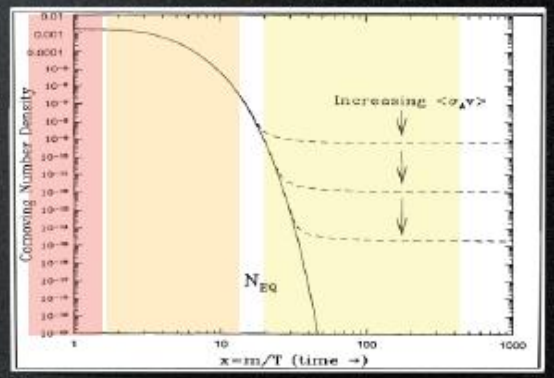

Introduction-02

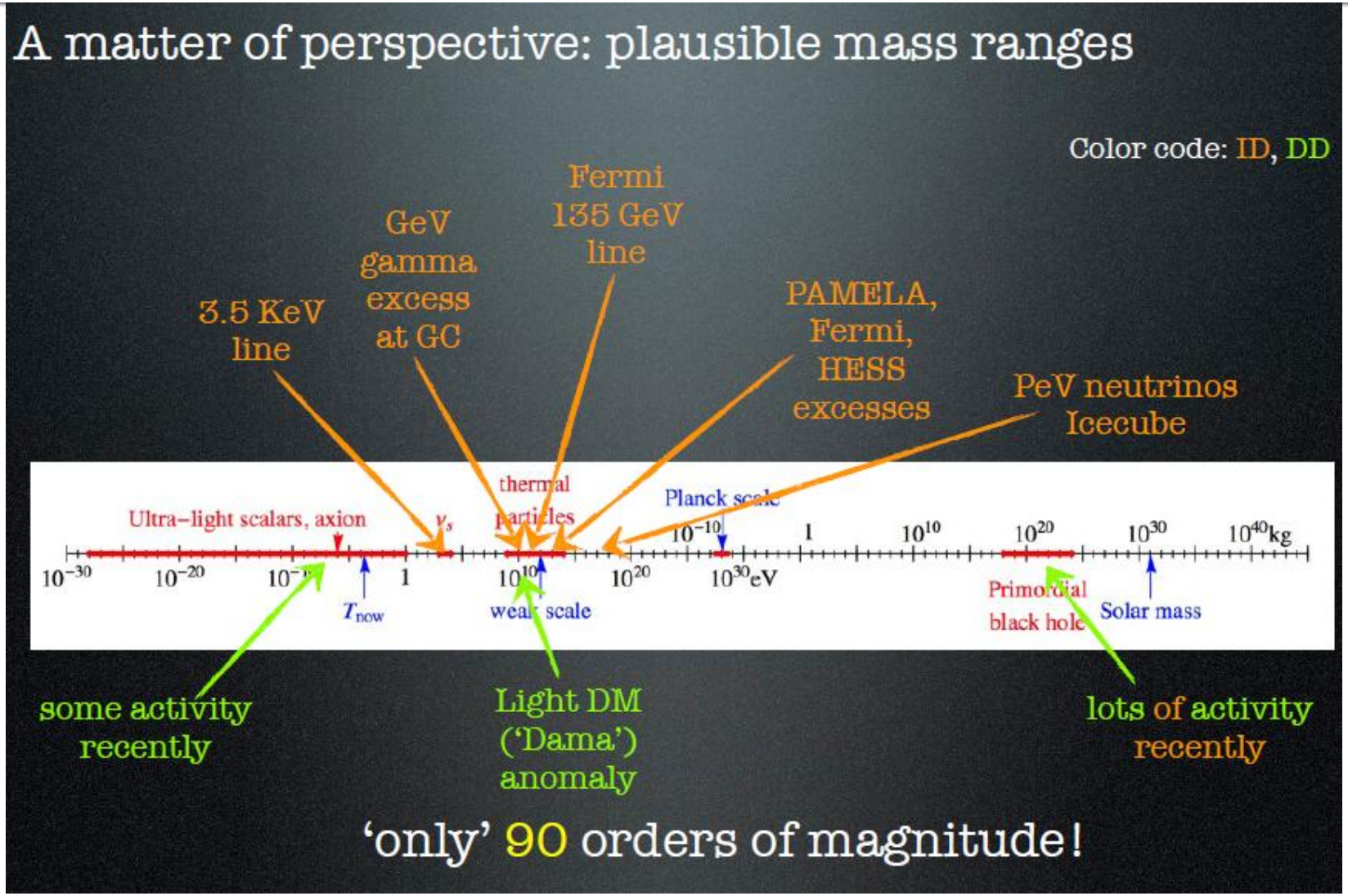

Introduction-03

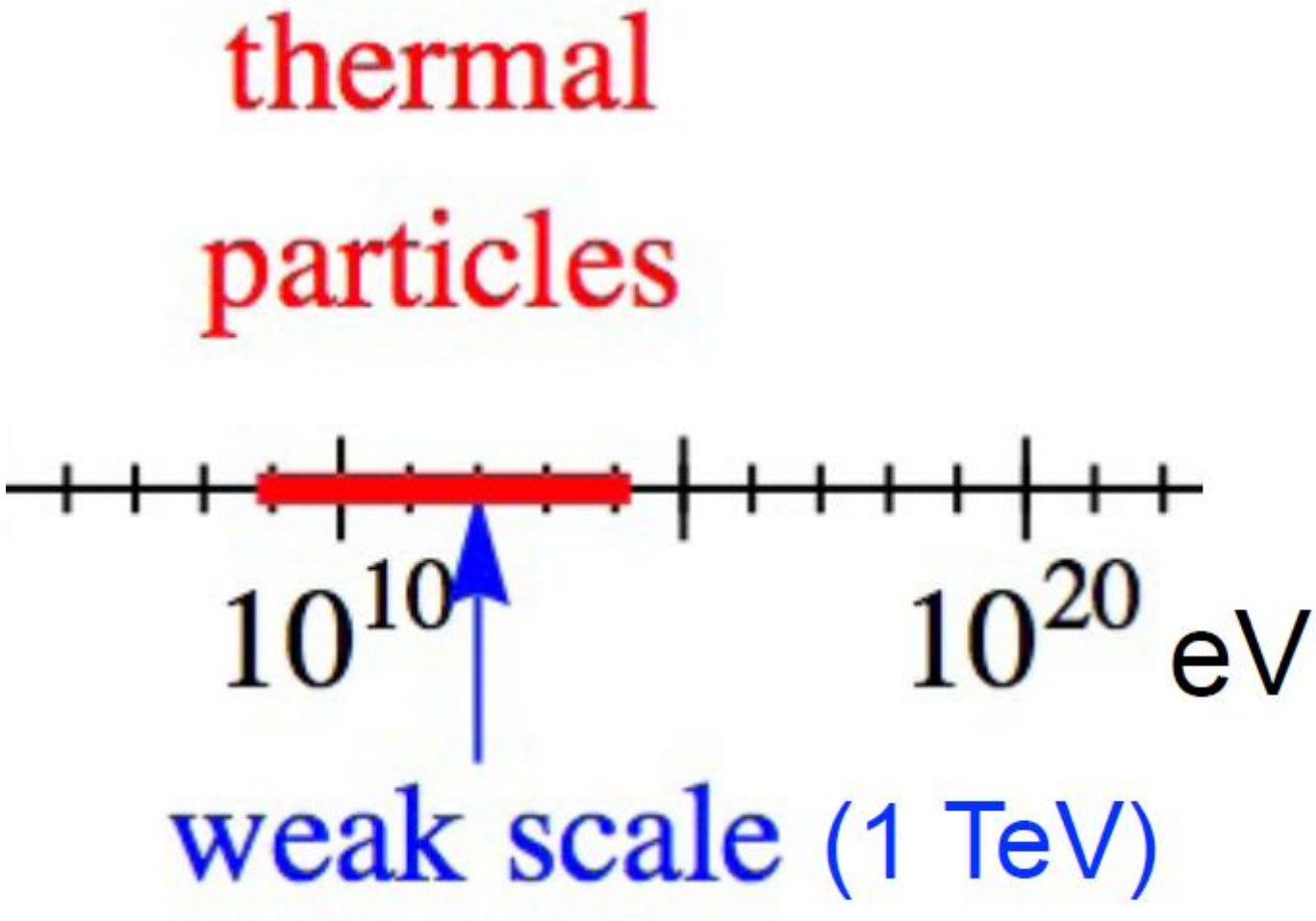

Dark-Matter Search:

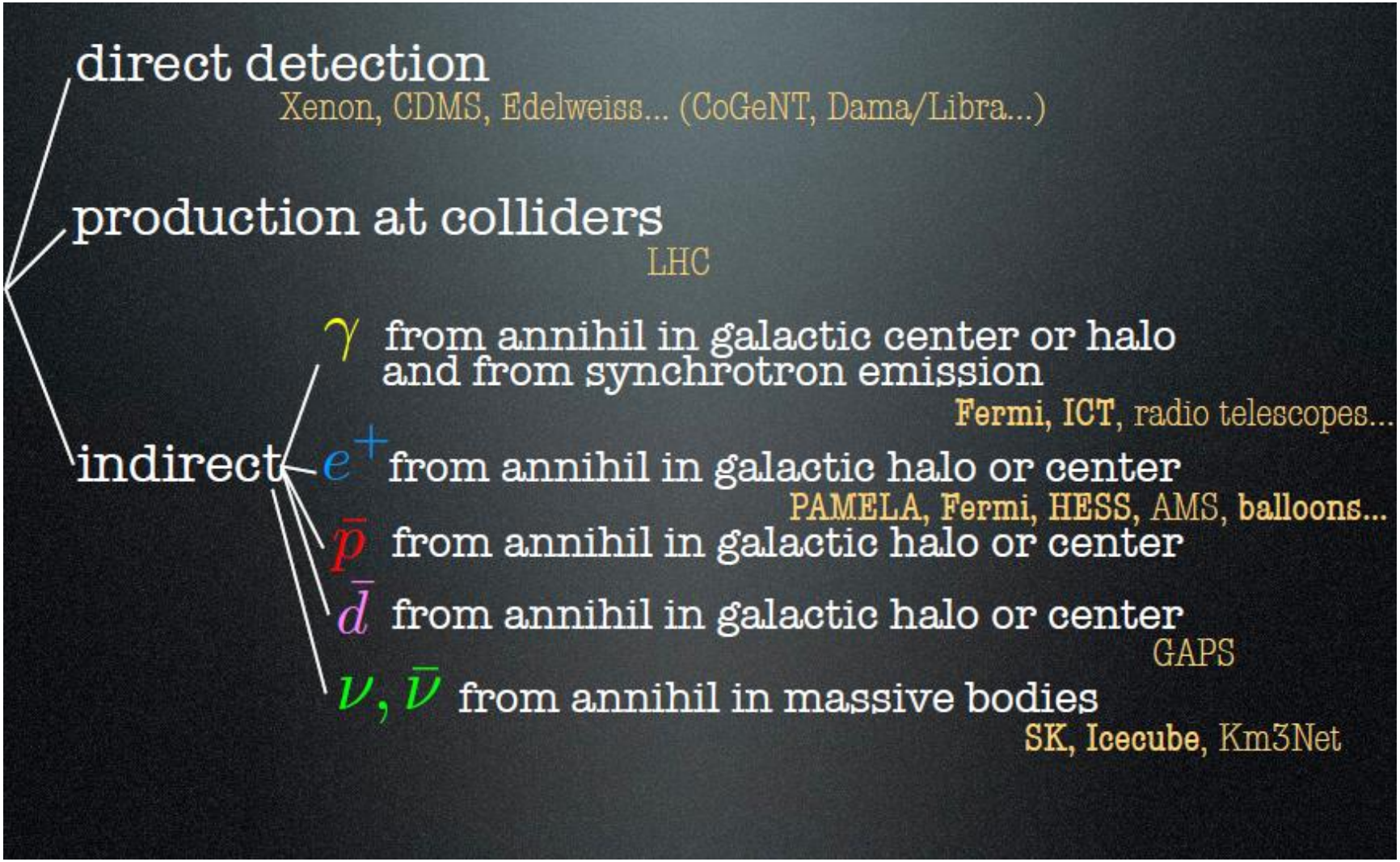

Primary Cosmic Ray Sources:

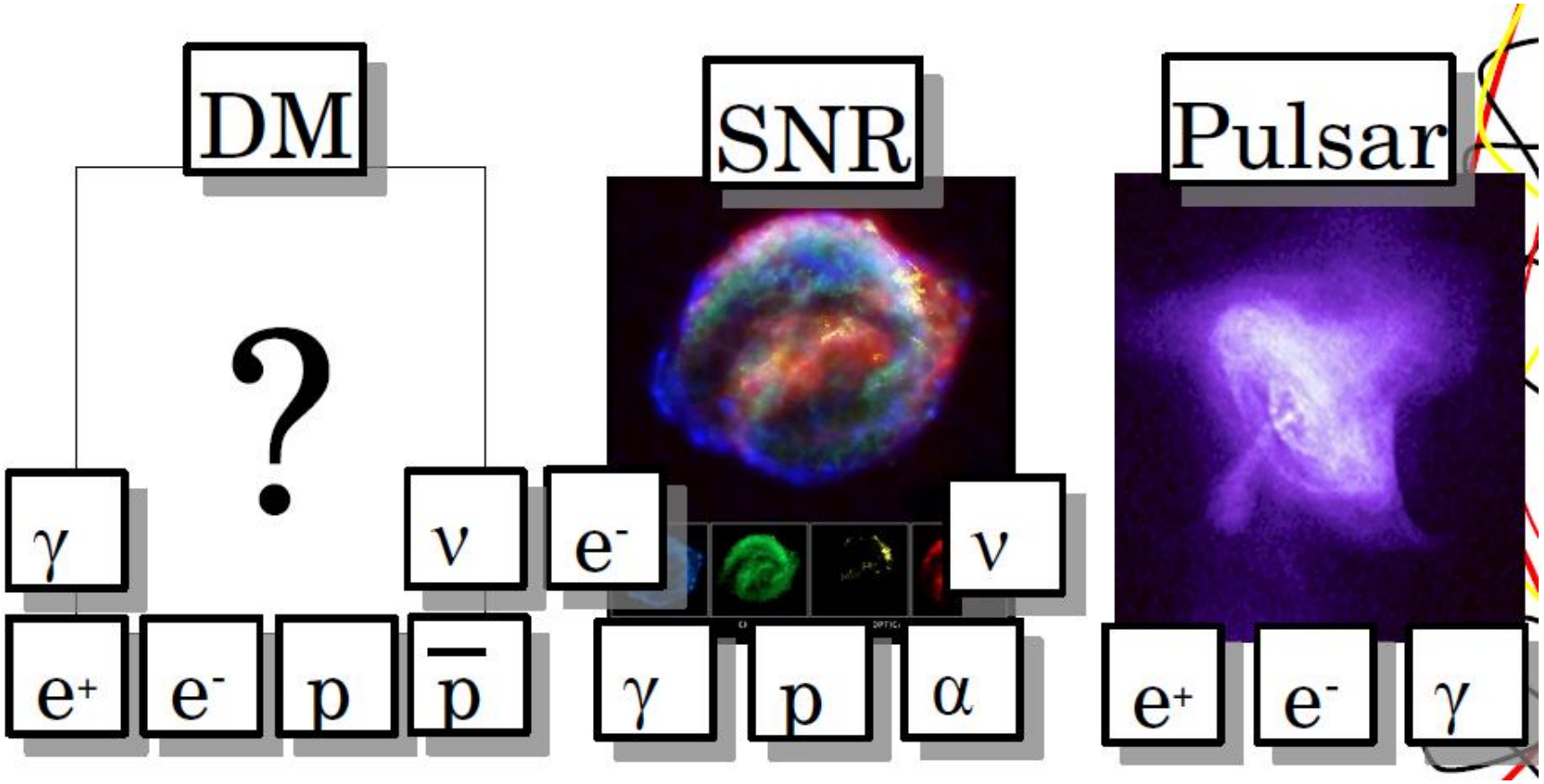

PAMELA and AMS design goal performance:

(GeV-TeV Energy Range)

Particle	Energy range for PAMELA	Energy range for AMS-02
$\bar{p}$	80 MeV - 190 GeV	up to 400 GeV
e^+	50 MeV - 270 GeV	up to 400 GeV
e^-	up to 400 GeV	around 1 TeV
p	up to 700 GeV	around a few TeV
$e^+ + e^-$	up to 2 TeV	around 1 TeV
Light nuclei ($Z \leq 6$)	up to 200 GeV/n	around a few TeV
Light isotopes (D, ^{3}He)	up to 1 GeV/n	up to 8 GeV/n
Antinuclei search	sensitivite to 10^{-7} in $\overline{\text{He}}$/He	10^{-9} in $\overline{\text{He}}$/He

Basic Ingredients of the CR Physics

- Most studies of GeV Galatic Cosmic Rays (GCR) nuclei assume a steady state/continous distribution for the sources of cosmic rays, but this distributions is actually discrete in time and in space.
- A stady-state model describes well many nuclei data (Ex: GALPROF).
- The Current progress in our understanding of CR physics (Acceleration, Propagation), the required consistency in explaining several GCRs manifestation (nuclei, gamma,…) as well as the precision of present and future space mission (e.g.. INTEGRAL, AMS, AGILE, GLAST) point towards the necessity to go beyond this approximation (steady-state model)

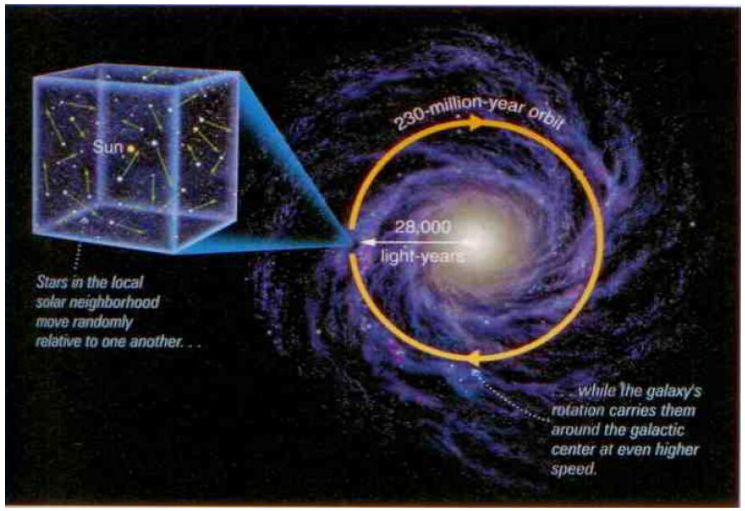

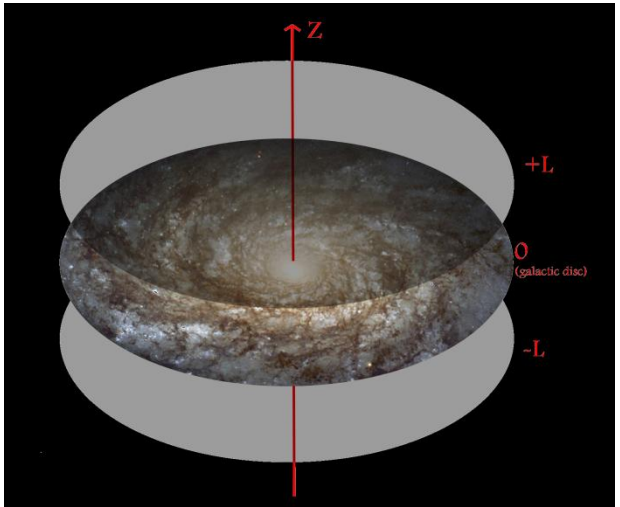

Diffusion and Transport of Cosmic Ray

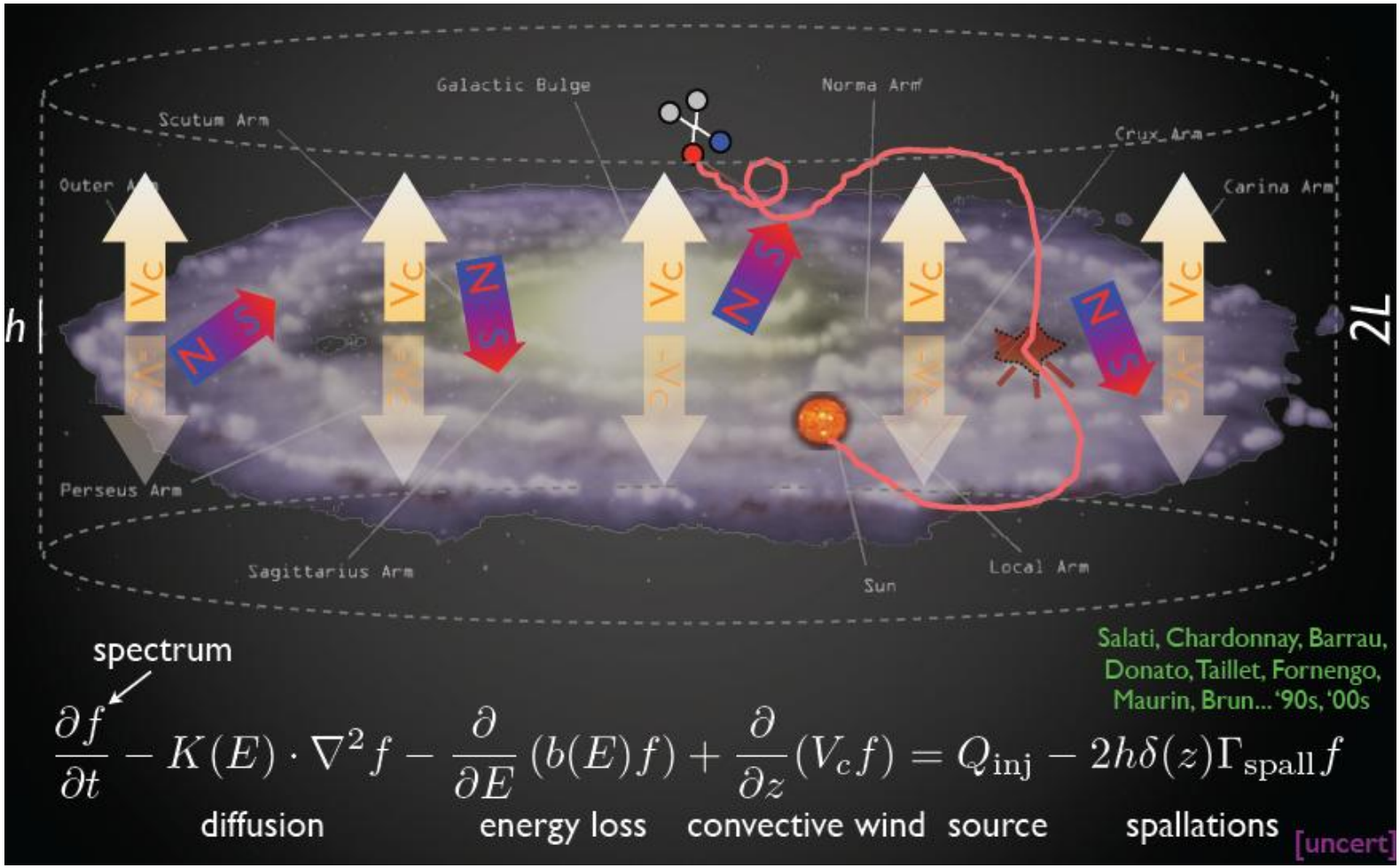

Cosmic Ray Transport:

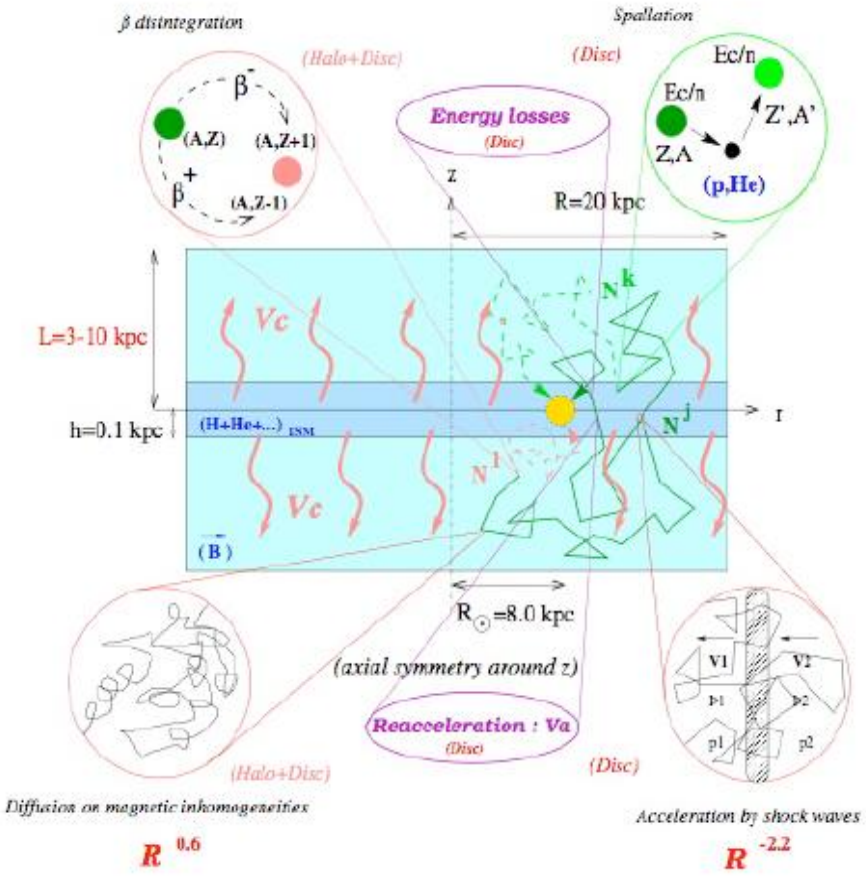

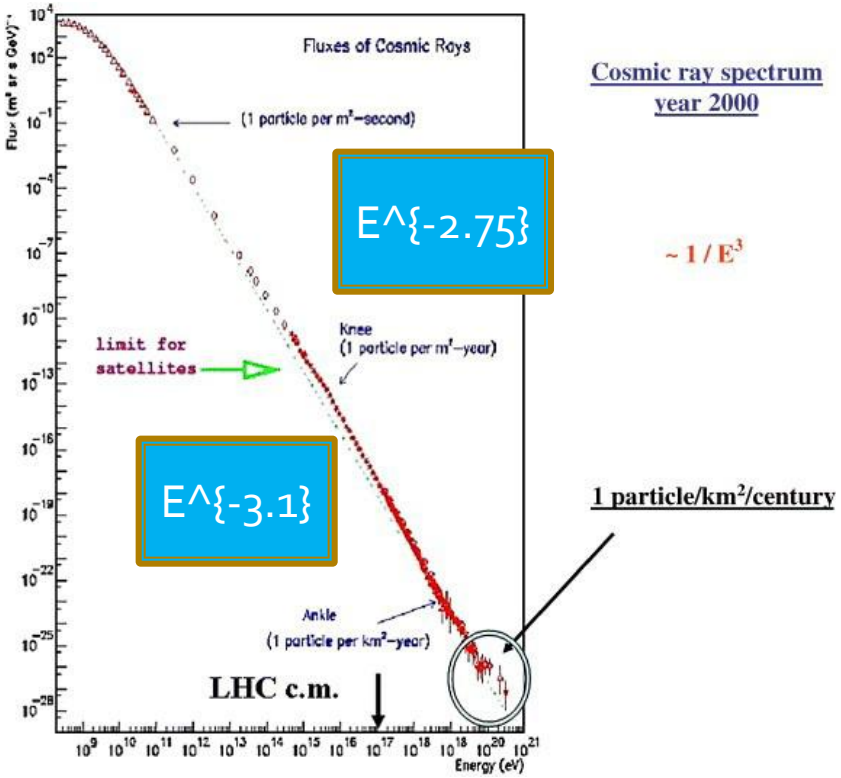

Our New Method: Green Ftn Method (A new paradigm of cosmic rays)

- Instead of the assumption on the homogenous steady-state sources of the cosmic ray inside the galaxy, we consider the importance of the discreteness of the sources which treat SN explosions as point-like events.
- We investigate the Green Function method instead of the Bessel function.
- Master equation:

$$\frac{\partial \varphi}{\partial t} + \partial_z (V_C \varphi) - K \Delta \varphi = q_{eff} = q_{acc} - q_{col}; \qquad \varphi \equiv dn_p / dT_p$$

$q_{acc}(x_S, t_S) = \Sigma q_i \ \delta^3(x_S - x_i)\ \delta(x_S - t_i)$: production rate of CR protons through acc.

$q_{col}(x_S, t_S) = 2h\ \delta(z_S)\ \Gamma_p\ \varphi(x_S, t_S)$: collisions of CR protons on the hydrogen and Helium atoms

with $\Gamma_p = \upsilon_p \times (\sigma_{pH} n_H + \sigma_{pHe} n_{He})$: collision rate

- Green Function for the CR protons:

$$G_p(x, t \leftarrow x_S, t_S) = \frac{1}{4\pi K \tau} \exp[-\frac{\rho^2}{4K\tau}] \times v_p(z, t \leftarrow z_S, t_S)$$

where $\tau = (t - t_S)$ and $\rho^2 = (x - x_S)^2 + (y - y_S)^2$

$$\frac{\partial v_p}{\partial t} + \partial_z (V_C v_p) - K \partial_z^2 v_p + 2h\delta(z)\Gamma_p v_p = \delta(z - z_S)\delta(t - t_S):$$ Vertical Propagator

Summary of our method:

- We compute the proton and helium spectra within the usual framework or diffusive propagation, and using propagation parameters consistent with B/C spectra, while taking into account the known local sources of cosmic rays. In our analysis, we don't need to modify the conventional CR propagation model.
- We use the known data of supernova remnants (SNR) and pulsars which can be found in the Green catalog (2009) and the ATNF pulsar database (Manchester et al. 2005).
- In order to show the lower-energy(power-law regime) and high energy(spectral hardening) part of the CR spectra to be connected with each other, a consistent treatment of the problem require that the proton and helium fluxes are calculated over the entire energy range.
- A crucial problem is also to understand why just a few local sources could explain the spectral hardening at high energies whereas the bulk of the Galatic sources is required to explain the power-law behavior of the fluxes below 250 GeV/n

Results:

model	K_0 [kpc^2/yr]	δ	L [kpc]	V_c [kpc/yr]	$q_{\rm p}^0$ [GeV^{-1}]	$q_{\rm He}^0$ [(GeV/n)$^{-1}$]
A	2.4×10^{-9}	0.85	1.5	1.38×10^{-8}	1.17×10^{52}	3.22×10^{51}
B	2.4×10^{-9}	0.85	1.5	1.38×10^{-8}	0.53×10^{52}	1.06×10^{51}
MED	1.12×10^{-9}	0.7	4	1.23×10^{-8}	15.8×10^{51}	3.14×10^{51}
model	$\alpha_{\rm p} + \delta$	$\alpha_{\rm He} + \delta$	ν [century^{-1}]	H injection	He injection	χ^2/dof
A	2.9	2.8	0.8	0.19	0.05	0.61
B	2.85	2.7	1.4	0.12	0.07	1.09
MED	2.85	2.7	0.8	0.148	0.07	1.3

Table 1. Sets of CR injection and propagation parameters discussed in the text.

Ex) Result for Model A: Best Chi-Square fit

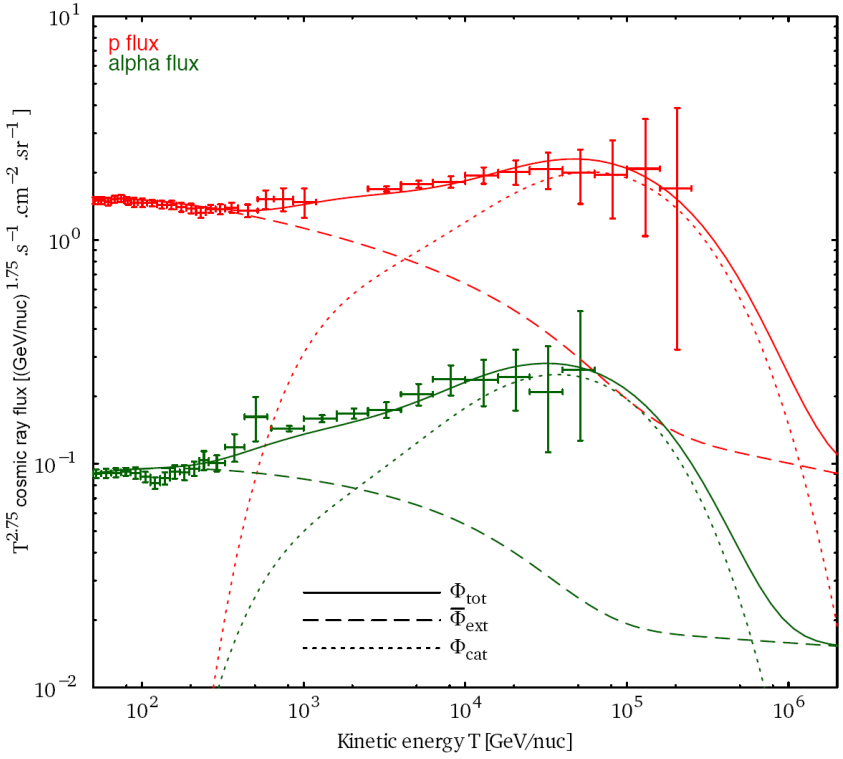

Fig. 1. Proton (upper curve) and helium (lower curve) spectra in the range extending from 50 GeV/nuc to 100 TeV/nuc, for the propagation parameters of model A (see Table 1), giving the best fit to the PAMELA (Adriani et al. 2011) and CREAM (Ahn et al. 2010) data : supernovae explosion rate $\nu = 0.8$ century^{-1}. Solid lines show the total flux, short-dashed lines show the flux due to the sources of the catalog, and the long-dashed curve the flux due to the rest of the sources.

Positron and Anti-proton Flux

Positron

- Background of secondary positron is produced by the spallation of the interstellar medium by impinging high-energy particles.
- Energy loss term becomes important, via synchrotron emission and inverse compton for > 10 GeV.
- Dominant mechanism:

$$p + \mathrm{H} \rightarrow \mathrm{X} + \pi^{\pm}$$
$$\pi^{\pm} \rightarrow \nu_{\mu} + \mu^{\pm}$$
$$\mu^{\pm} \rightarrow \nu_{\mu} + \nu_{\mathrm{e}} + \mathrm{e}^{\pm}$$

- Dark matter annihilation:

$$\chi + \chi \rightarrow q\bar{q},\ W^{+}W^{-},\ \ldots\ldots \rightarrow \bar{p},\ \bar{D},\ e^{+},\ \gamma\ \&\ \nu_{s}$$

Total flux:

$$\Phi_{e^{+}}^{tot} = \Phi_{\mathrm{e}^{+}}^{\mathrm{sec}} + \Phi_{\mathrm{e}^{+}}^{\mathrm{DM}}$$

Production of antimatter in the Galaxy

Antiproton

- The spallation of high-energy primary nuclei impinging on the atoms of the interstellar medium inside the galactic disc produces secondary antiprotons.
- The annihilation of DM candidate particles throughout the Milky Way halo generates primary antiprotons. Notice that WIMP annihilations take place all over the diffusive halo.
- Tertiary antiprotons result from the inelastic and non-annihilating interactions with a nucleon at rest. The energy transfer may be sufficient to excite it as a Δ resonance. This mechanism redistributes antiprotons toward lower energies and flattens their spectrum.
- Antiprotons may also annihilate on interstellar H and He.

Obsevation data (positron): AMS02-April 2013

Aguilar et al. (AMS02 collaboration), PRL 110, 141102 (2013)

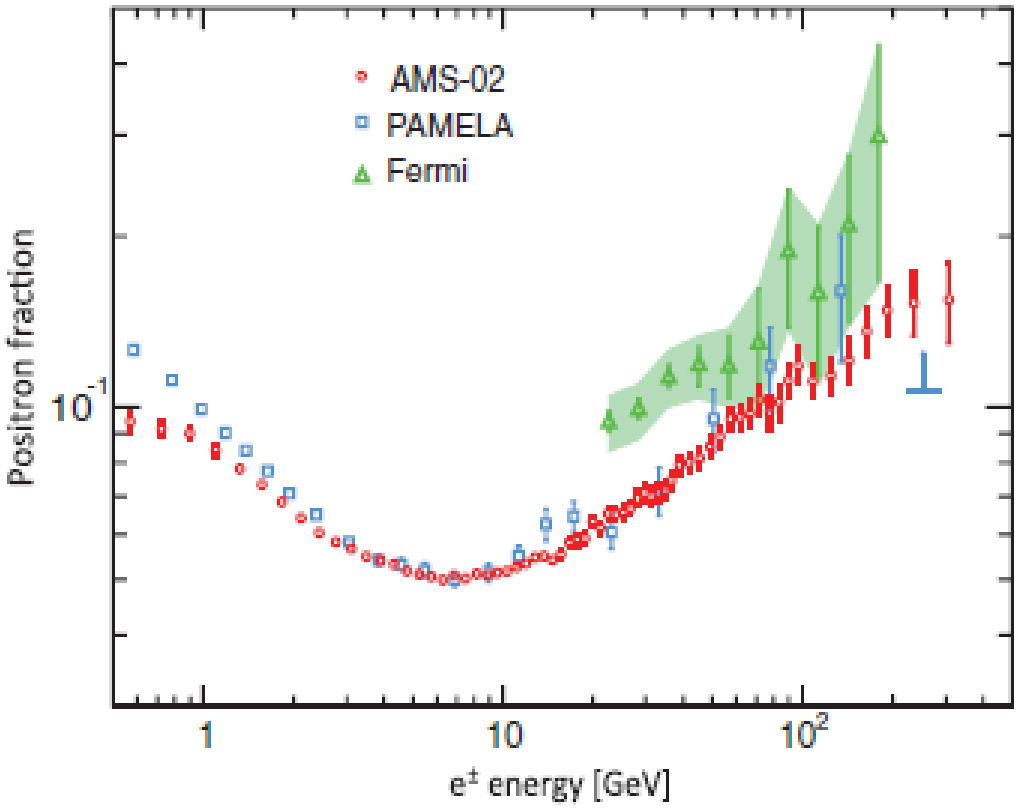

Indirect Detection: Basics

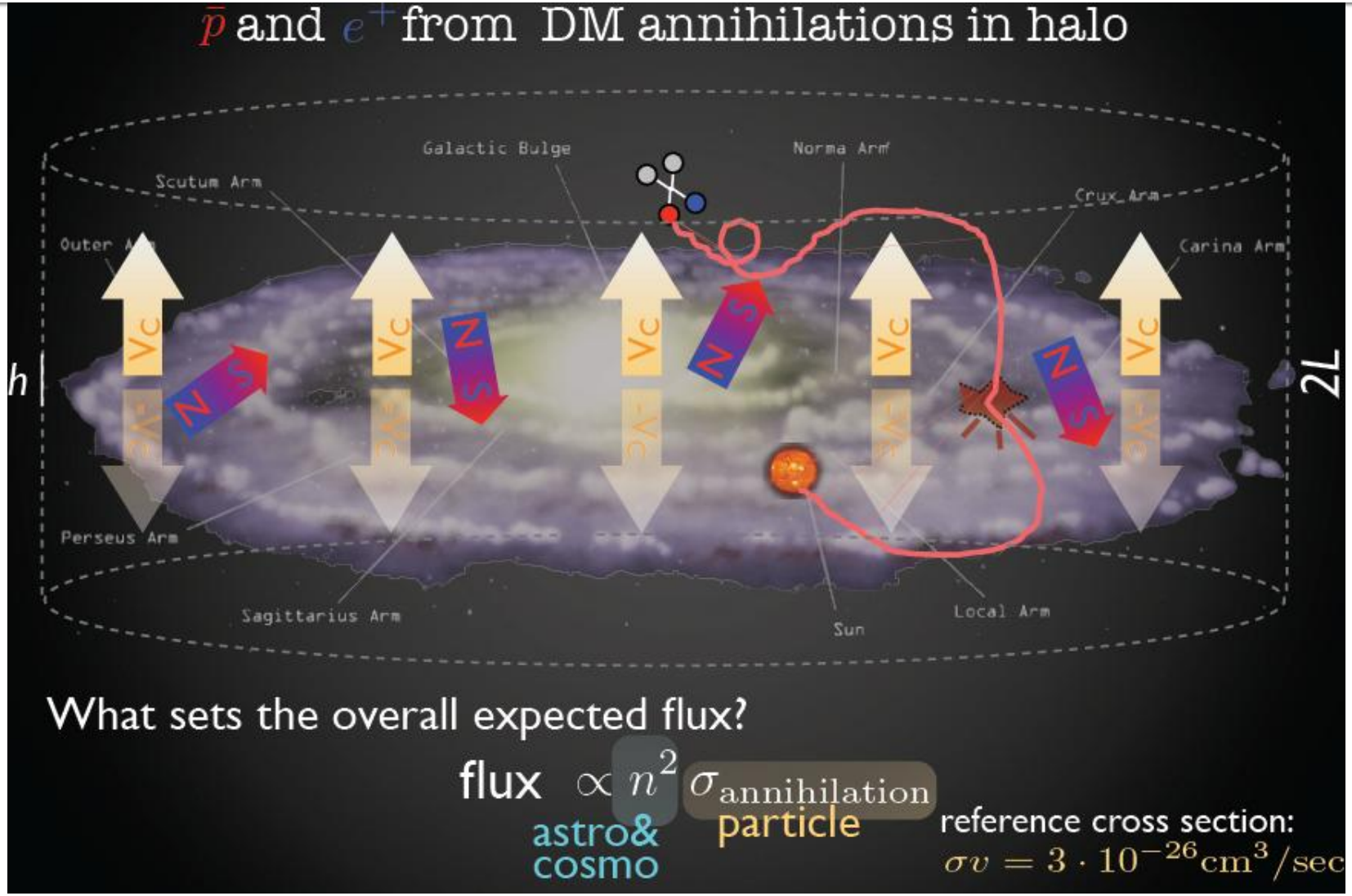

Indirect Detection: Basics

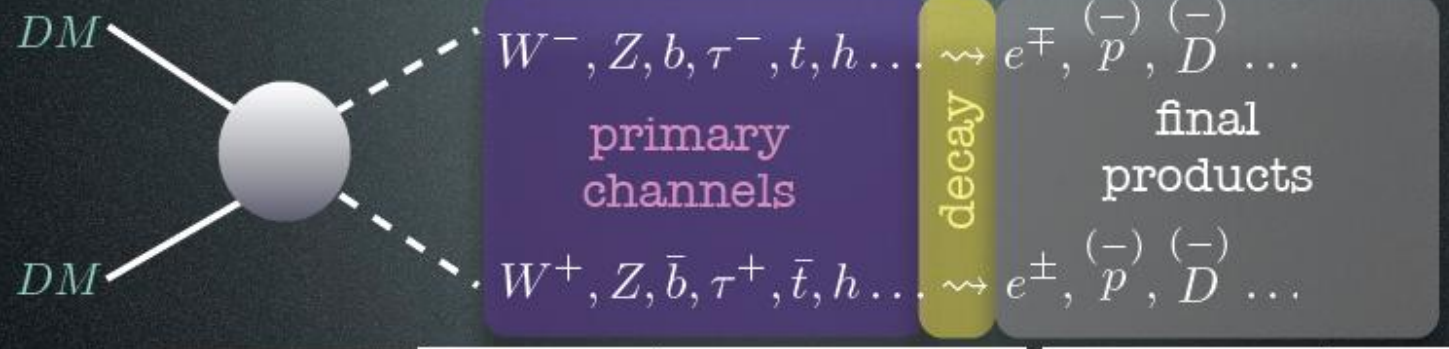

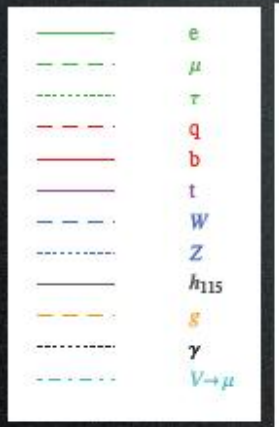

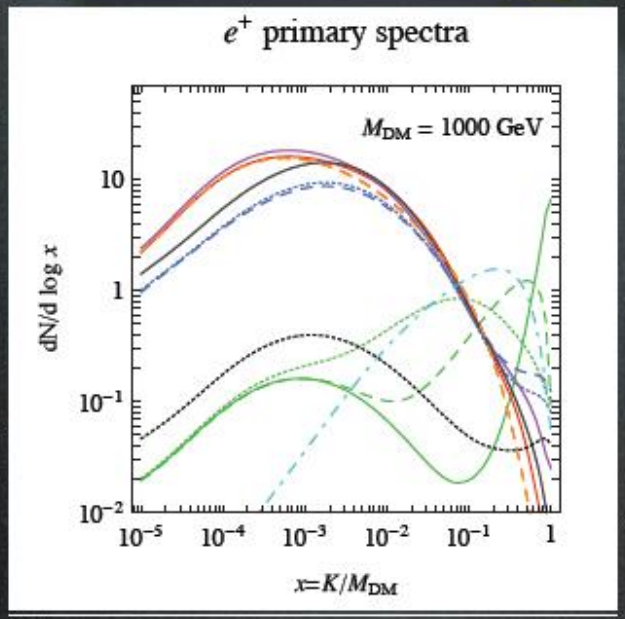

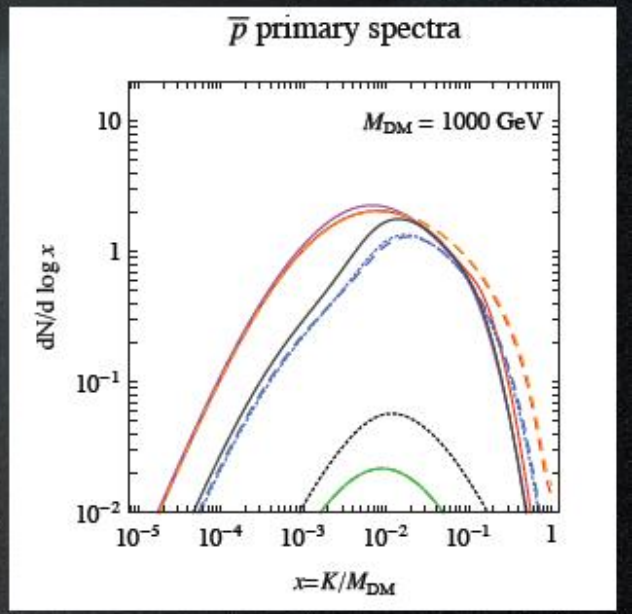

So what are the particle physics parameters?

1. Dark Matter mass
2. primary channel(s)

Positrons and Electrons

positron fraction

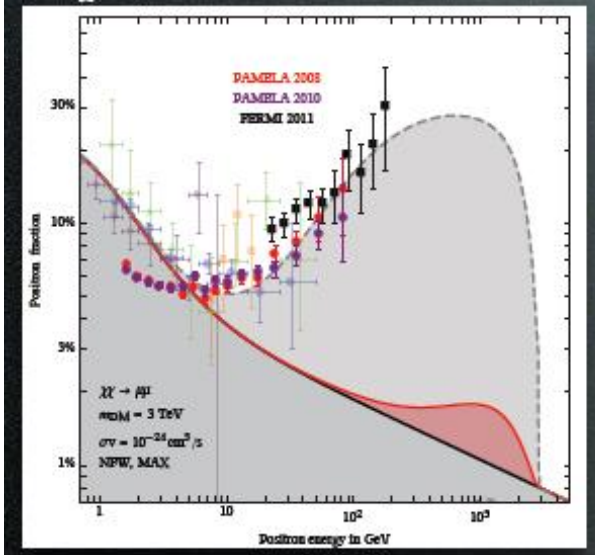

antiprotons

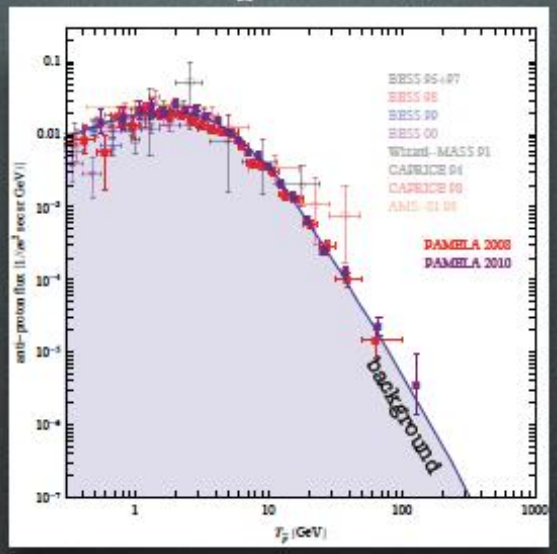

electrons + positrons

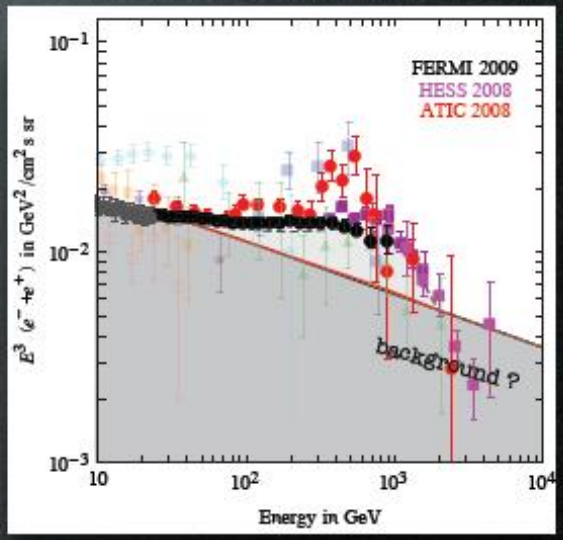

Are these signals of Dark Matter?

YES: few TeV, leptophilic DM
with huge $\langle \sigma v \rangle \approx 10^{-23}\ \mathrm{cm}^3/\mathrm{sec}$

NO: a formidable 'background' for future searches

Post AMS02 data - 2013

positron fraction

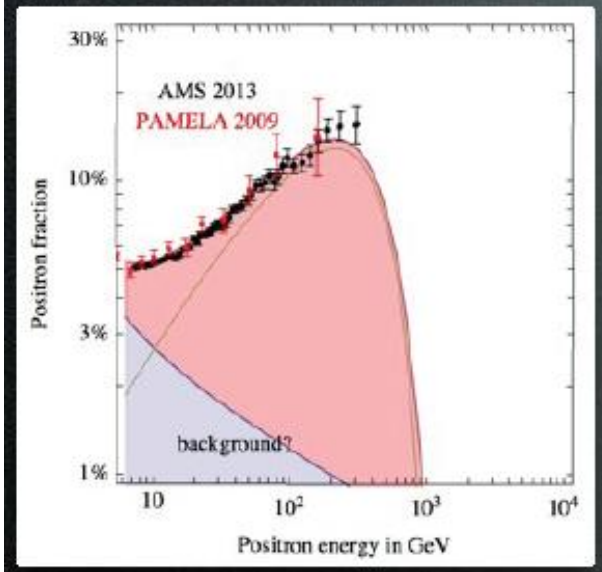

antiprotons

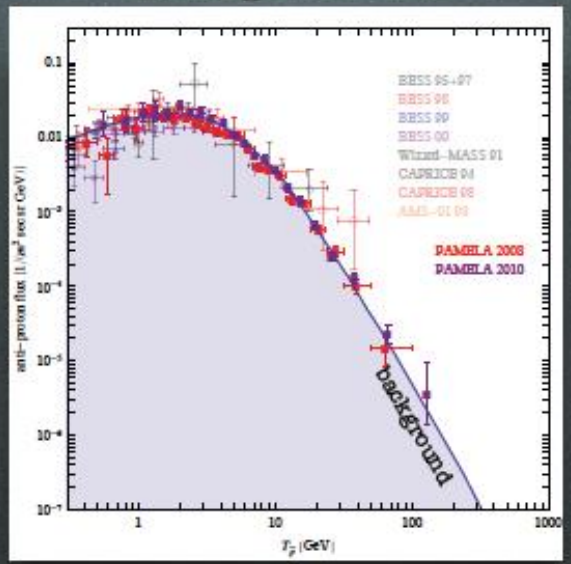

electrons + positrons

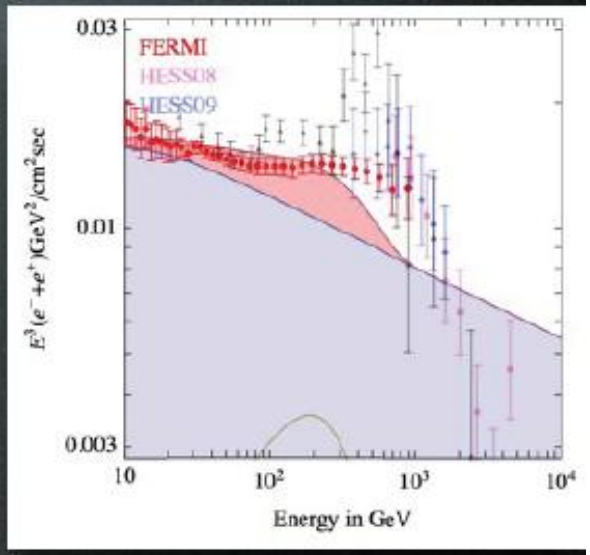

Are these signals of Dark Matter?

YES: one TeV, leptophilic DM
with huge $\langle \sigma v \rangle \approx 10^{-23}\ \mathrm{cm}^3/\mathrm{sec}$
'tension' between positron frac and $e^+ + e^-$

Enhencement ?

How to reconcile $\sigma = 3 \cdot 10^{-26} \mathrm{cm}^3/\mathrm{sec}$ with $\sigma \simeq 10^{-23} \mathrm{cm}^3/\mathrm{sec}$?

- DM is produced non-thermally: the annihilation cross section today is unrelated to the production process

	at freeze-out	*today*
- astrophysical boost	no clumps	clumps
- resonance effect	off-resonance	on-resonance
- Sommerfeld effect	$v/c \simeq 0.1$	$v/c \simeq 10^{-3}$

Model Building:

- Minimal extensions of the SM:
  heavy WIMPS (Minimal DM, Inert Doublet)

  Cirelli, Strumia et al. 2005-2009 Tytgat et al. 0901.2556

- More drastic extensions:
  New models with a rich Dark sector

  M.Pospelov and A.Ritz, 0810.1502: Secluded DM - A.Nelson and C.Spitzer, 0810.5167: Slightly Non-Minimal DM - Y.Nomura and J.Thaler, 0810.5397: DM through the Axion Portal - R.Harnik and G.Kribs, 0810.5557: Dirac DM - D.Feldman, Z.Liu, P.Nath, 0810.5762: Hidden Sector - T.Hambye, 0811.0172: Hidden Vector - K.Ishiwata, S.Matsumoto, T.Moroi, 0811.0250: Superparticle DM - Y.Bai and Z.Han, 0811.0387: sUED DM - P.Fox, E.Poppitz, 0811.0399: Leptophilic DM - C.Chen, F.Takahashi, T.T.Yanagida, 0811.0477: Hidden-Gauge-Boson DM - E.Ponton, L.Randall, 0811.1029: Singlet DM - S.Baek, P.Ko, 0811.1646: U(1) Lmu-Ltau DM - I.Cholis, G.Dobler, D.Finkbeiner, L.Goodenough, N.Weiner, 0811.3641: 700+ GeV WIMP - K.Zurek, 0811.4429: Multicomponent DM - M.Ibe, H.Murayama, T.T.Yanagida, 0812.0072: Breit-Wigner enhancement of DM annihilation - H.Chun, J.-O.Park, 0812.0308: sub-GeV hidden U(1) in GMSB - M.Lattanzi, J.Silk, 0812.0360: Sommerfeld enhancement in cold substructures - M.Pospelov, M.Trott, 0812.0432: super-WIMPs decays DM - Zhang, Bi, Liu, Liu, Yin, Yuan, Zhu, 0812.0522: Discrimination with SR and IG - Liu, Yin, Zhu, 0812.0964: DMnu from GC - M.Pohl, 0812.1174: electrons from DM - J.Hisano, M.Kawasaki, K.Kohri, K.Nakayama, 0812.0219: DMnu from GC - R.Allahverdi, B.Dutta, K.Richardson-McDaniel, Y.Santoso, 0812.2196: SuSy B-L DM - S.Hamaguchi, K.Shirai, T.T.Yanagida, 0812.2374: Hidden-Fermion DM decays - D.Hooper, A.Stebbins, K.Zurek, 0812.3202: Nearby DM clump - C.Delaunay, P.Fox, G.Perez, 0812.3331: DMnu from Earth - Park, Shu, 0901.0720: Split-UED DM - .Gogoladze, R.Khalid, Q.Shafi, H.Yuksel, 0901.0923: cMSSM DM with additions - Q.H.Cao, E.Ma, G.Shaughnessy, 0901.1334: Dark Matter: the leptonic connection - E.Nezri, M.Tytgat, G.Vertongen, 0901.2556: Inert Doublet DM - J.Mardon, Y.Nomura, D.Stolarski, J.Thaler, 0901.2926: Cascade annihilations (light non-abelian new bosons) - P.Meade, M.Papucci, T.Volansky, 0901.2925: DM sees the light - D.Phalen, A.Pierce, N.Weiner, 0901.3165: New Heavy Lepton - T.Banks, J.-F.Fortin, 0901.3578: Pyrma baryons - K.Bae, J.-H. Huh, J.Kim, B.Kyae, R.Viollier, 0812.3511: electrophilic axion from flipped-SU(5) with extra spontaneously broken symmetries and a two component DM with Z_8 parity - ...

- Decaying DM

  Ibarra et al., 2007-2009 Nardi, Sannino, Strumia 0811.4153

  A.Arvanitaki, S.Dimopoulos, S.Dubovsky, P.Graham, R.Harnik, S.Rajendran, 0812.2075

Model Building:

- Minimal extensions of the SM:
  heavy WIMPS (Minimal DM, Inert Doublet)

  Cirelli, Strumia et al. 2005-2009 Tytgat et al. 0901.2556

- More drastic extensions:
  New models with a rich Dark sector
  - TeV mass DM
    - new forces (that Sommerfeld enhance)
      - leptophilic because: - kinematics (light mediator)
                             - DM carries lepton #

- Decaying DM

  Ibarra et al., 2007-2009 Nardi, Sannino, Strumia 0811.4153

  A.Arvanitaki, S.Dimopoulos, S.Dubovsky, P.Graham, R.Harnik, S.Rajendran, 0812.2075

Pulsar Scenario:

Unlike in DM hypothesis, Pulsar scenario does not require the introduction of an extra, exotic component to explain data.

Pulsar are undisputed source of electron-positron pairs, produced in the neutron star magnetosphere and, possibly, re-accelerated by the pulsar wind and/or in SNR shocks. Nearby pulsars, the local flux of high energy electrons and positrons is very likely dominant.

The recent PAMELA and AMS02 data can rather well be interpreted as originating from one single nearby Pulsar or by the coherent superposition of the electron and positron flux from all galatic pulsars.

Two Pulsar Parameters:

Spectral index and the total energy of positron flux

Positron spectrum

$$g(E) = Q_0 \left(\frac{E_0}{E}\right)^{\gamma} \exp(-E/E_C)\,.$$

Total energy of positron flux

$$\int_{E_{\min}}^{+\infty} E_S\, g(E_S)\, dE_S = f W_0\,.$$

$$t_\star \equiv t - t_S = \int_E^{E_\star} \frac{dE'}{b(E')}\,. \qquad b(E) = \frac{E_0}{\tau_E}\,\epsilon^2\,,$$

$$G_{e^+}(\mathbf{x}, t, E \leftarrow \mathbf{x}_S, t_S, E_S) = \frac{b(E_\star)}{b(E)}\,\tilde{G}(\mathbf{x} \leftarrow \mathbf{x}_S; \lambda_D)\,\delta(E_S - E_\star)\,,$$

$$\Phi^{\rm psr}_{e^+}(\odot, E) = \frac{c}{4\pi}\,\frac{b(E_\star)}{b(E)}\,\tilde{G}\left\{\mathbf{x} \leftarrow \mathbf{x}_\star; \lambda_D(E, E_\star)\right\} g(E_\star)\,,$$

* Positron fraction [10 GeV < E < 100 GeV]: $\Phi_{e^+} \propto \exp(-d^2 / \lambda_D^2)$
* Positron sphere radius: $\lambda_D \approx 4\,K_0\,t_*\,(E/E_0)^{\delta}$
* Lower energy limit: $E_{\min} = E_0 (d^2 / 4K_0\,t_*)^{1/\delta}$

Nearby Pulsar catalog (ATNF):

Table 3. Results for the pulsar parameters fW_0 and γ for the best fits in the single pulsar approach. Only pulsars with a p-value > 0.0455, taking their distance uncertainty into account, are listed, besides the well-known pulsars Monogem and Vela. The bold lines correspond to the nominal distance value.

Name	Age [kyr]	Distance [kpc]	fW_0 [10^{34} GeV]	γ	χ^2	χ^2_{dof}	p
J1745−3040	546	0	$(2.95 \pm 0.07) \cdot 10^{-3}$	1.45 ± 0.02	23.4	0.57	0.99
		0.20	$\mathbf{(3.03 \pm 0.06) \cdot 10^{-3}}$	$\mathbf{1.54 \pm 0.02}$	**33.6**	**0.82**	**0.79**
		1.3	1	2.54	9902	241	0
J0633+1746 *Geminga*	342	0.17	$(1.48 \pm 0.03) \cdot 10^{-3}$	1.56 ± 0.02	26.8	0.65	0.96
		0.25	$\mathbf{(1.63 \pm 0.02) \cdot 10^{-3}}$	$\mathbf{1.68 \pm 0.02}$	**49.6**	**1.21**	**0.17**
		0.48	$(1.01 \pm 0.06) \cdot 10^{-2}$	2.29 ± 0.02	332	8.10	0
J0942−5552	461	0.10	$(2.28 \pm 0.05) \cdot 10^{-3}$	1.48 ± 0.02	21.7	0.53	0.99
		0.30	$\mathbf{(2.61 \pm 0.04) \cdot 10^{-3}}$	$\mathbf{1.69 \pm 0.02}$	**61.0**	**1.49**	**0.02**
		1.1	1	2.65	7747	189	0
J1001−5507	443	0	$(2.13 \pm 0.05) \cdot 10^{-3}$	1.46 ± 0.02	19.8	0.48	0.99
		0.30	$\mathbf{(2.49 \pm 0.03) \cdot 10^{-3}}$	$\mathbf{1.70 \pm 0.02}$	**62.4**	**1.52**	**0.02**
		1.4	1	2.46	13202	322	0
J1825−0935	232	0.1	$(0.80 \pm 0.02) \cdot 10^{-3}$	1.52 ± 0.02	21.0	0.51	0.99
		0.30	$\mathbf{(1.45 \pm 0.03) \cdot 10^{-3}}$	$\mathbf{1.94 \pm 0.02}$	**126**	**3.07**	**0**
		1.0	1	2.64	12776	312	0
J0659+1414 *Monogem*	111	0.25	$(1.06 \pm 0.05) \cdot 10^{-3}$	2.18 ± 0.02	216	5.27	0
		0.28	$\mathbf{(2.53 \pm 0.16) \cdot 10^{-3}}$	$\mathbf{2.37 \pm 0.02}$	**316**	**7.71**	**0**
		0.31	$(7.96 \pm 0.61) \cdot 10^{-3}$	2.58 ± 0.02	444	10.8	0
J0835+4510 *Vela*	11.3	0.26	$(2.53 \pm 0.08) \cdot 10^{-1}$	3	14316	349	0
		0.28	$\mathbf{(3.90 \pm 0.14) \cdot 10^{-1}}$	**3**	**14982**	**365**	**0**
		0.3	$(6.00 \pm 0.26) \cdot 10^{-1}$	3	15446	377	0

Best fit

Worst fit

Failed

Pulsar Analysis (Geminga)

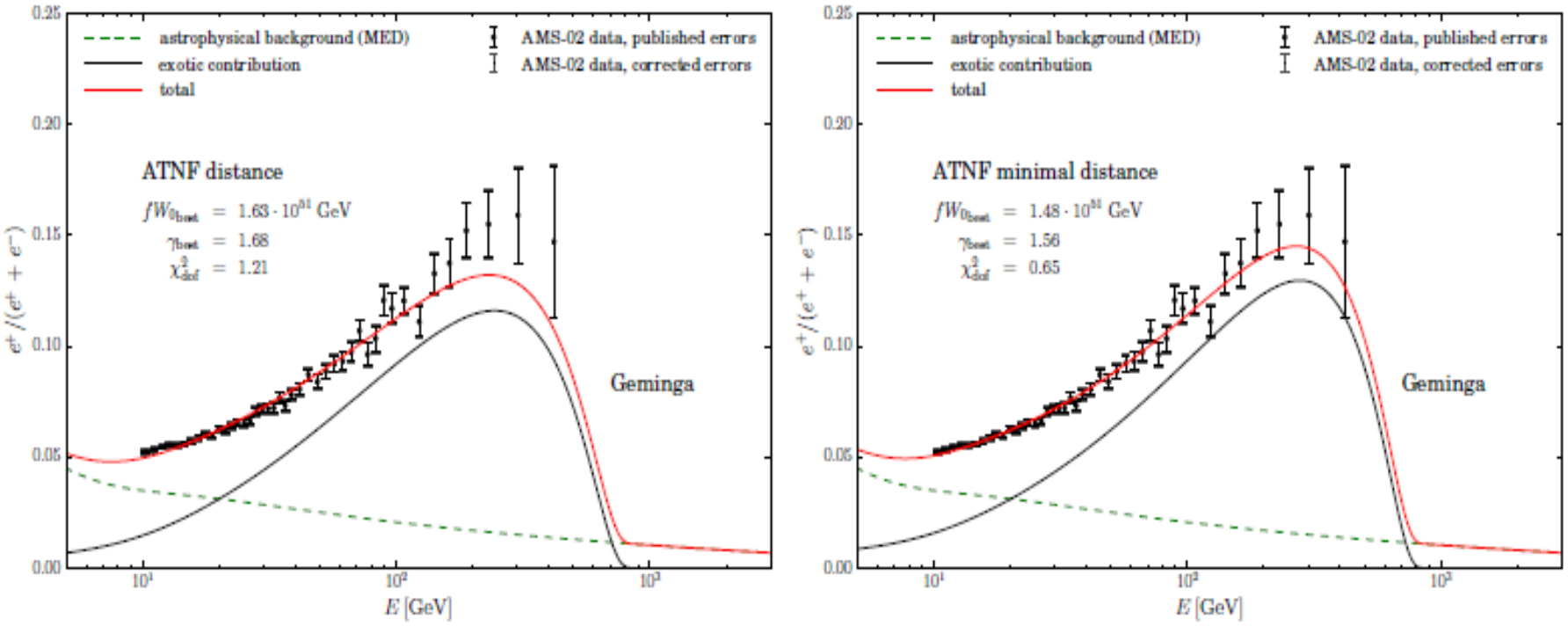

Fig. 11. Positron fraction for the best fits for the pulsar Geminga considering the nominal (left panel) and minimal (right panel) distances. The spectral index γ at the source decreases with the pulsar distance. The positron flux becomes harder and better fits the highest-energy data points.

Pulsar Analysis (J1745-3040)

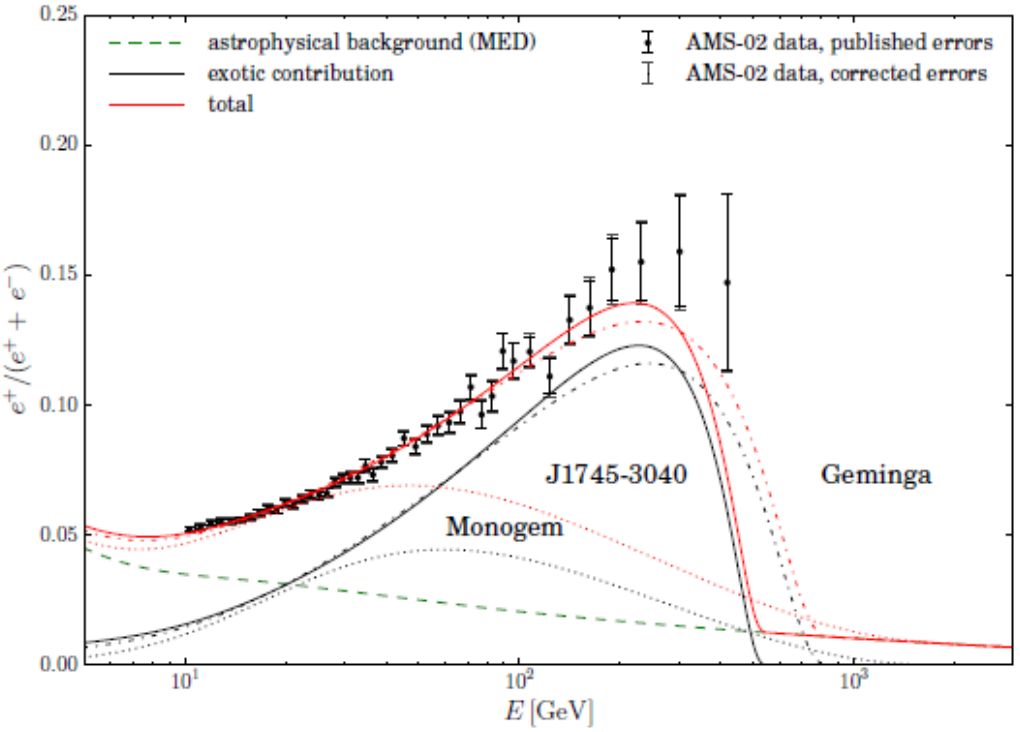

Fig. 12. Positron fraction for the best fits for the pulsars J1745-3040 (solid line), Geminga (dashed-dotted line), and Monogem (dotted line) with the propagation model MED.

Discussions & Conclusions:

- We resolve the anomaly of Proton/Helium flux of the cosmic ray nuclei of the CREAM-PAMELA data, and Positron Excess at PAMELA and AMS02 by considering the importance of the local sources of the supernovae remnants (SNR) and pulsars.
- We find the importance of the young, energetic and nearby SNRs and pulsars, and their contributions.
- Green Function method will be used widely in the analysis of Future experiments (e.g. INTEGRAL, AMS, GLAST, ….).
- Monogram, vela can't adjust the AMS02-data:
  Very young age → can't contribute to the low energy positron fraction (10 GeV < E < 50 GeV)

Future Projects during 2014-2016

- focused on the effect of discrete sources of primary CRs on secondary species:
  (ex: positron, antiproton and anti-deuteron, …).

- Could the positron flux and the antiproton flux at the earth depend on significantly the discreteness of CR sources?

- Can we explain within the same scheme both the PAMELA-CREAM anomaly of the TeV scale cosmic rays of nuclei and the anomaly of PAMELA-AMS02 anomaly of the positron excess ? → on going research.

Thanks for your attention !

Back up Slides

A) Anomaly in P, He CR-spectra:

CREAM Data 2010-11: APJ 728,122 (2011)

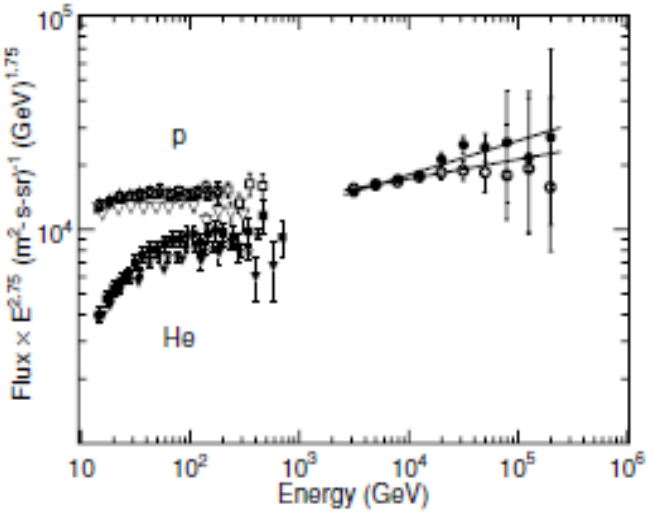

Figure 3. Measured energy spectra of cosmic-ray protons and helium nuclei. The CREAM-I spectra are compared with selected previous measurements (Alcaraz et al. 2000; Haino et al. 2004; Boezio et al. 2003) using open symbols for protons and filled symbols for helium: CREAM (circles), AMS (stars), BESS (squares), CAPRICE (inverted triangles). The error bars represent one standard deviation, which is not visible when smaller than the symbol size. The lines represent power-law fits to the CREAM data.

The Astrophysical Journal, 728:122 (8pp), 2011 February 20

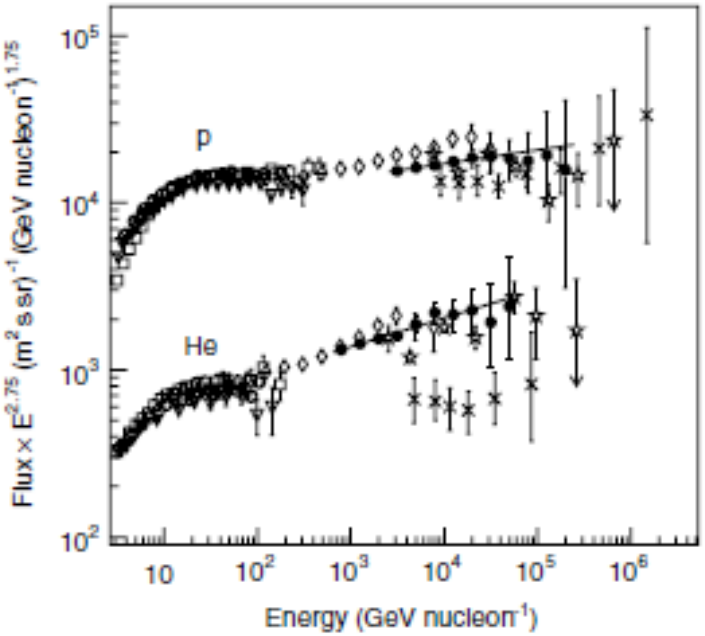

Figure 3. CREAM proton and helium differential $Flux \cdot E^{2.75}$ in GeV nucleon^{-1} at the top of the atmosphere. The CREAM proton and helium spectra (filled circles) are shown together with previous measurements: BESS (squares), CAPRICE98 (downward triangles), AMS (open circles), ATIC-2 (diamonds), JACEE (stars), and RUNJOB (crosses). The lines represent power-law fits with spectral indices of -2.66 ± 0.02 for protons and -2.58 ± 0.02 for helium nuclei, respectively.

Anomaly in P, He CR-spectra:

PAMELA 2011: Science 332,69 (2011)

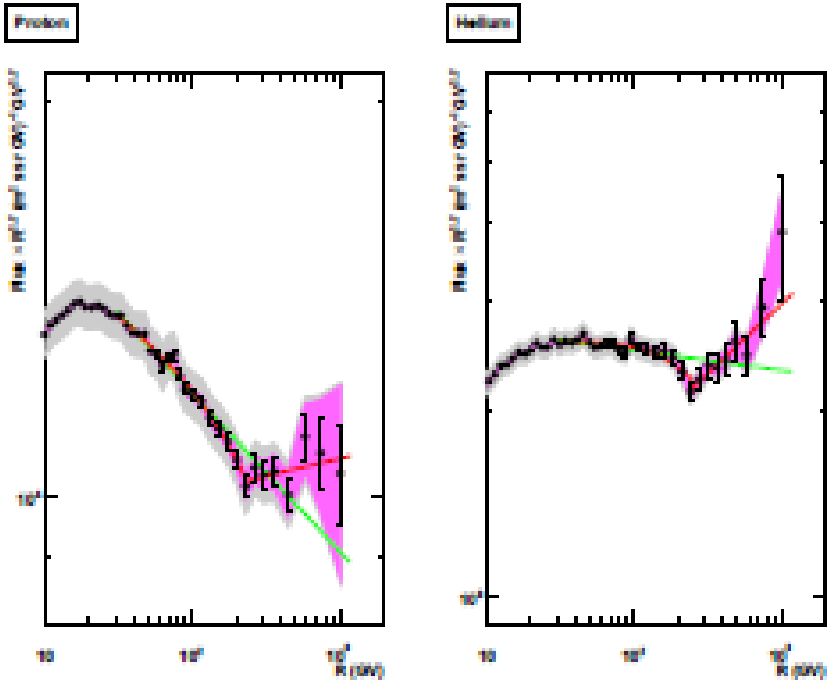

Figure 4: Proton (left panel) and helium (right panel) spectra in the range 10 GV - 1.2 TV. The grey shaded area represents the estimated systematic uncertainty, the pink shaded area represents the contribution due to tracker alignment. The straight (green) lines represent fits with a single power law in the rigidity range 30 GV - 240 GV. The red curves represent the fit with a rigidity dependent power law (30-240 GV) and with a single power law above 240 GV.

Anomaly in P, He CR-spectra:
Confirmed by AMS02: PRL 114, 2015

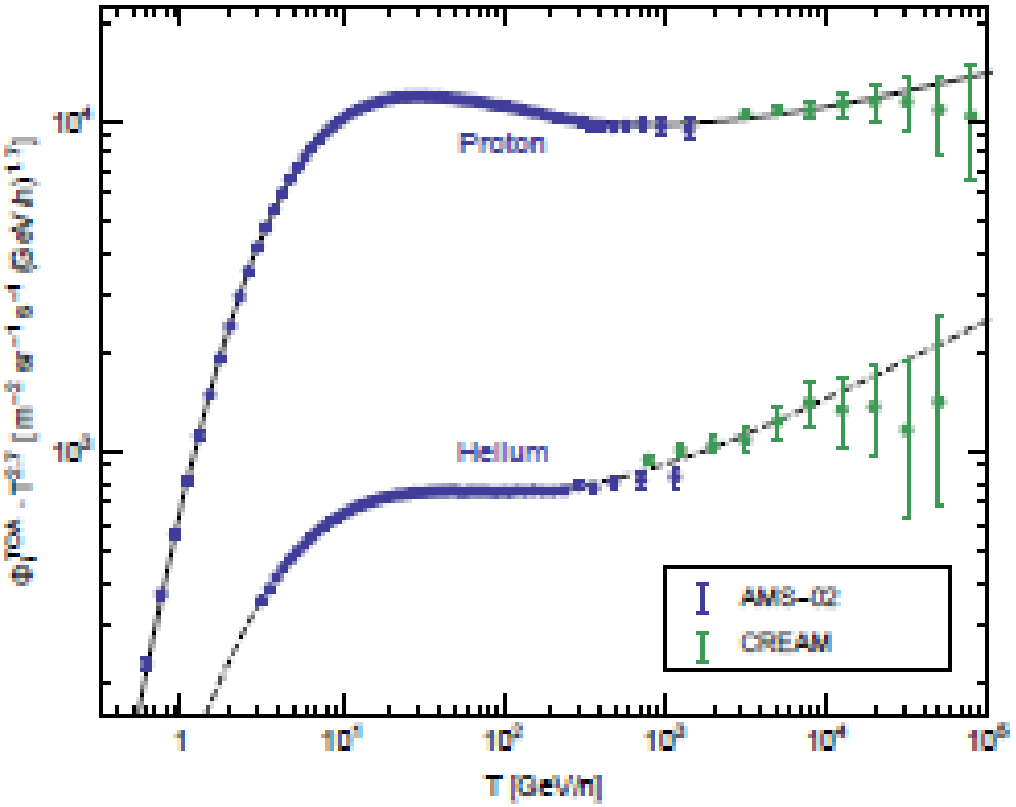

PAMELA-CREAM Anomaly (2010-present)

- Precise measurements of nuclei fluxes are needed to understand the acceleration and subsequent propagation of cosmic rays in the Galaxy.
- Discrepant hardenings in the TeV scale cosmic ray proton-Helium nuclei spectra was appeared in 2011.
- CREAM-PAMELA experiments found that the spectral shapes of proton and helium above 250 GeV/nucleon are different and can not be well described by a single power law: Cosmic flux ~ E^{-2.75}
- Single power law model is rejected at 95% C.L. and rejected at 99.7% C.L. by the Fisher's and Student's t-tests.

- For Proton: hardening occures at 232^{+35}_{-30} GeV/nucleon

$$\gamma^{R}_{80-232,p} = 2.85 \pm 0.015 \pm 0.004 \quad ; \quad \gamma^{R}_{>232,p} = 2.67 \pm 0.03 \pm 0.05$$

- For Helium at 243^{+27}_{-31} GeV/nucleon

$$\gamma^{R}_{80-240,He} = 2.766 \pm 0.01 \pm 0.027 \quad ; \quad \gamma^{R}_{>243,He} = 2.477 \pm 0.06 \pm 0.03$$

Basic Ingredients of the CR Physics

- Most studies of GeV Galatic Cosmic Rays (GCR) nuclei assume a steady state/continous distribution for the sources of cosmic rays, but this distributions is actually discrete in time and in space.
- A stady-state model describes well many nuclei data (Ex: GALPROF).
- The Current progress in our understanding of CR physics (Acceleration, Propagation), the required consistency in explaining several GCRs manifestation (nuclei, gamma,…) as well as the precision of present and future space mission (e.g.. INTEGRAL, AMS, AGILE, GLAST) point towards the necessity to go beyond this approximation (steady-state model)

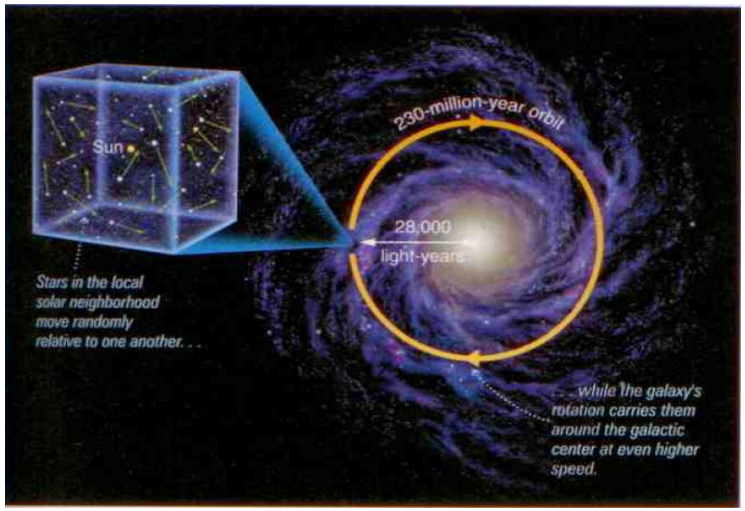

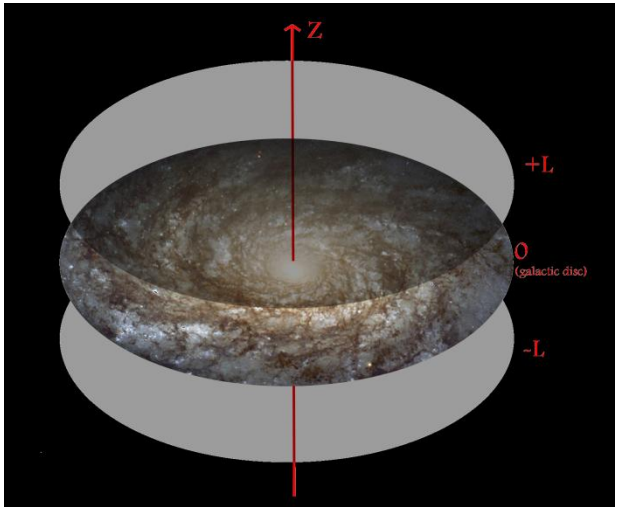

Diffusion and Transport of Cosmic Ray

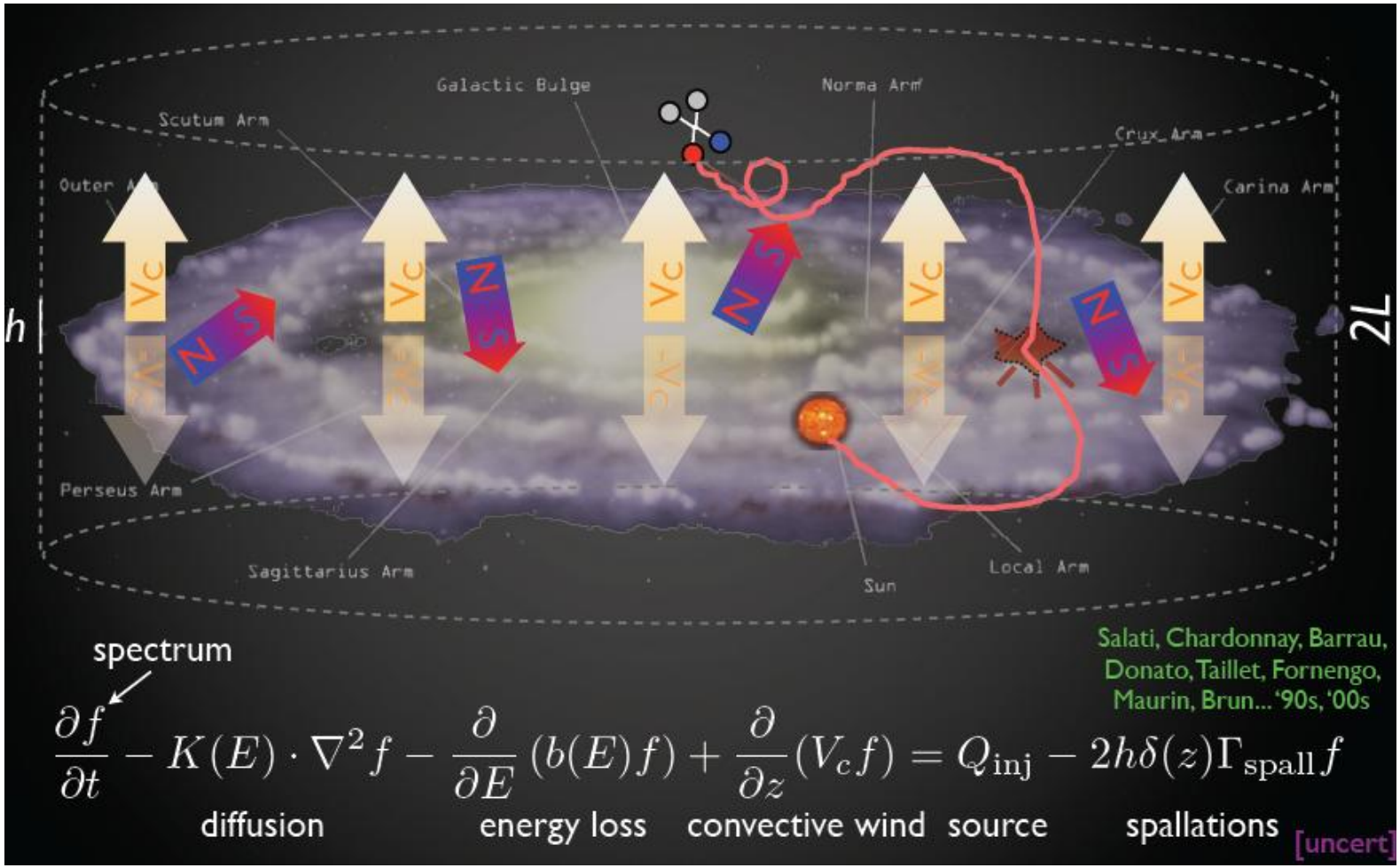

Cosmic Ray Transport and Diffusion

- General Diffusive Equation of CRs.

$$\partial_t \Psi + \vec{\nabla} \cdot (\vec{V_c} \Psi - K \vec{\nabla} \Psi) + \partial_E (b_{loss} \Psi - D_{EE} \partial_E \Psi) = Q - D$$

a) Time-dependence: since the global structure of the Galaxy seems quite stable for the billions of years, and the time scale of CR which we are interested in a few million years, the first term can be neglected except for the cosmic ray density Ψ and the source term Q in specific cases.

b) Convection term: There are observations that galatic winds exist in outer galaxies, they are probably due to stellar winds, supernova explosions, and probably cosmic ray themselves.

$\vec{V_c} = V_c \, \widehat{e_z \, \sigma(z)}$: sensitive to low energy CR

c) Diffusion term: because the exact structure of the Galatic magnetic field is very unclear and so are the models relating this structure to the diffusion parameter K. Diffusion will be considered homogeneous over the complete diffusion halo.

$K(r, E, t) = K_0 \beta \, \Re^{\delta}$ ($\Re$=particle rigidity: p/Ze)

continues:

- General Diffusive Equation of CRs.

$$\partial_t \Psi + \vec{\nabla} \cdot (\vec{V_c} \Psi - K \vec{\nabla} \Psi) + \partial_E (b_{loss} \Psi - D_{EE} \partial_E \Psi) = Q - D$$

d) Energy losses: $b_{loss} = b(E) = \frac{E_0}{\tau_E} \varepsilon^2; \quad \varepsilon = \frac{E}{E_0 = 1GeV}$: mainly comes from the inverse-compton

e) Energy diffusion: Random magnetohydrodynamical waves can lead to stochastic acceleration of CR, but the proper microscopic description is not easy. Describing the process requires to know the collision rate and the speed of the waves: Alfven velocity $\vec{V_a}$.

$$D_{EE} = \frac{2}{9} V_a^2 \frac{E^2 \beta^4}{K(E)}$$

f) Source term and Distruction term

Old method:
Steady State and the Bessel Ftn solution

$$\psi(r,z) = \sum_{i=1}^{+\infty} P_i(z)\ \mathrm{J}_0(\alpha_i\ \mathrm{r/R_{gal}})$$

Master Equation: ($\partial_t \psi = 0$)

$$\partial_z(V_c\ \psi)\ -\mathrm{K}\,\Delta\psi + 2\,\mathrm{h}\,\delta(z)\,\Gamma_\mathrm{p}\,\psi = \mathrm{q_{acc}} = \mathrm{Q_p}\,D(r)\,2\,\mathrm{h}\,\delta(\mathrm{z})$$

$$D(r) = \sum_{i=1}^{+\infty} \mathrm{D_i}\ \mathrm{J}_0(\alpha_i\ \mathrm{r/R_{gal}})$$

$$P_i(z) = P_i(0)\ \exp[-\frac{V_\mathrm{C}\,|\,z\,|}{2\,\mathrm{K}}]\ \sinh\{\frac{S_i}{2}(L-|\,z\,|\}\ \Big/\ \sinh\{\frac{S_i}{2}L\}$$

$$\textit{with}\ \ S_i^2 = \left(\frac{2\alpha_i}{R_{gal}}\right)^2 + \left(\frac{V_C}{\mathrm{K}}\right)^2$$

Understanding of power-law behavior

- The energy spectrum of primary cosmic ray approximately behaves as E^{-2.75}, in the 10 GeV to 100 TeV range.

- This is rather well understood if one assumes that these cosmic rays are accelerated by energetic events such as supernova explosion shocks, distributed evenly in the disk of our Galaxy.
- Once injected inside the Galatic magnetic halo with a rate

$$q \propto R^{-\alpha} (R \equiv p/Ze : \text{Rigidity}) \text{ and } \alpha \simeq 2.15 \pm 0.15$$

- Particles are subsequently scattered by the turbulent irregularities of the Galatic magnetic field.
- Their transport is described by space diffusion with a coefficient

$$K \propto R^{\delta} (\delta \in [0.4,\ 0.85] \text{ from B/C ratio})$$

- At high energy, the flux of a given primary CR species at the Earth:
-

$$\Phi \propto q/K = E^{-(\alpha+\delta)}$$

Current Other Expanations

- Mainly modification of the energy behavior of either the injection spectrum q(E) or the diffusion coefficient K(E).
- A break in alpha could arise from a modification of the conventional diffusive shock acceleration (DSA) scheme:
  Ohira & Ioka(2011), Malkov et al.(2012)
- A different classes of CR sources: for instance, cosmic rays accelerated in the magnetized winds of exploding Wolf-Rayet and red supergiant stars could have a double spectrum, with a hard component produced in the polar cap regions of these objects: Stanev et al.(1993), Zatsepin & Sokolskaya(2006), Biermann et al.(2010), Yuan et al.(2011)
- Modification of the diffusion coefficient K(E): an expected decrease of the spectral index delta at high energy, or an unusual strong spallation of the CR species on the Galactic gas, but criticized in a detail analysis by Vladimirov et al.(2012):
  Ave et al.(2009), Blasi et al.(PRL:2012), Tomassetti(2012), Horandel et al.(2007), Blasi &Amato(2011)

Our New Method: Green Ftn Method (A new paradigm of cosmic rays)

- Instead of the assumption on the homogenous steady-state sources of the cosmic ray inside the galaxy, we consider the importance of the discreteness of the sources which treat SN explosions as point-like events.
- We investigate the Green Function method instead of the Bessel function.
- Master equation:

$$\frac{\partial \varphi}{\partial t} + \partial_z (V_C \varphi) - K \Delta \varphi = q_{eff} = q_{acc} - q_{col}; \qquad \varphi \equiv dn_p / dT_p$$

$q_{acc}(x_S, t_S) = \Sigma q_i \ \delta^3(x_S - x_i)\ \delta(x_S - t_i)$: production rate of CR protons through acc.

$q_{col}(x_S, t_S) = 2h\ \delta(z_S)\ \Gamma_p\ \varphi(x_S, t_S)$: collisions of CR protons on the hydrogen and Helium atoms

with $\Gamma_p = \upsilon_p \times (\sigma_{pH} n_H + \sigma_{pHe} n_{He})$: collision rate

- Green Function for the CR protons:

$$G_p(x, t \leftarrow x_S, t_S) = \frac{1}{4\pi K \tau} \exp[-\frac{\rho^2}{4K\tau}] \times v_p(z, t \leftarrow z_S, t_S)$$

where $\tau = (t - t_S)$ and $\rho^2 = (x - x_S)^2 + (y - y_S)^2$

$$\frac{\partial v_p}{\partial t} + \partial_z (V_C v_p) - K \partial_z^2 v_p + 2h\delta(z)\Gamma_p v_p = \delta(z - z_S)\delta(t - t_S):$$ Vertical Propagator

Solution of the vertical propagator:

- The final results of the vertical propagator is given by

$$\nu_p(z,t \leftarrow z_S,t_S) = \exp\{\frac{V_C(|z|-|z_S|)}{2K}\} \times \theta(\tau) \times [\sum_{n=1}^{\infty}\frac{1}{N_n}e^{-\alpha_n\tau}\varepsilon_n(z)\varepsilon_n(z_S) + \sum_{n=1}^{\infty}\frac{1}{N_n^{'}}e^{-\alpha_n^{'}\tau}\varepsilon_n^{'}(z)\varepsilon_n^{'}(z_S)]$$

where

$$\text{even eigenfunction:} \quad \varepsilon_n(z) = \sin\{k_n(L-|z|)\} \quad \text{with} \quad -\tan(k_nL) = k_n/(V_C/2K + h\Gamma_p/K)$$

$$\text{odd eigenfunction:} \quad \varepsilon_n^{'}(z) = \sin\{k_n^{'}(L-z)\} \quad \text{with} \quad k_n^{'}L = n\pi$$

$$\textit{and} \qquad \alpha = K\,k^2 + V_C^2/4K$$

When we impose the vertical boundary of the DH, the boundary acts as mirrors and give an infinite series of images from the source.

The n-th image is located at

z_n = 2 L n + (-1)^n z_s

$$\nu_p(z,t \leftarrow z_S,t_S) = \sum_{n=-\infty}^{+\infty}(-1)^n \frac{\theta(\tau)}{\sqrt{4\pi K\tau}}\exp\{-\frac{(z_n - z_S)^2}{4K\tau}\}$$

Local Catalog of SN and Pulsar:
(2 kpc around Earth and less than 30,000 years ago)

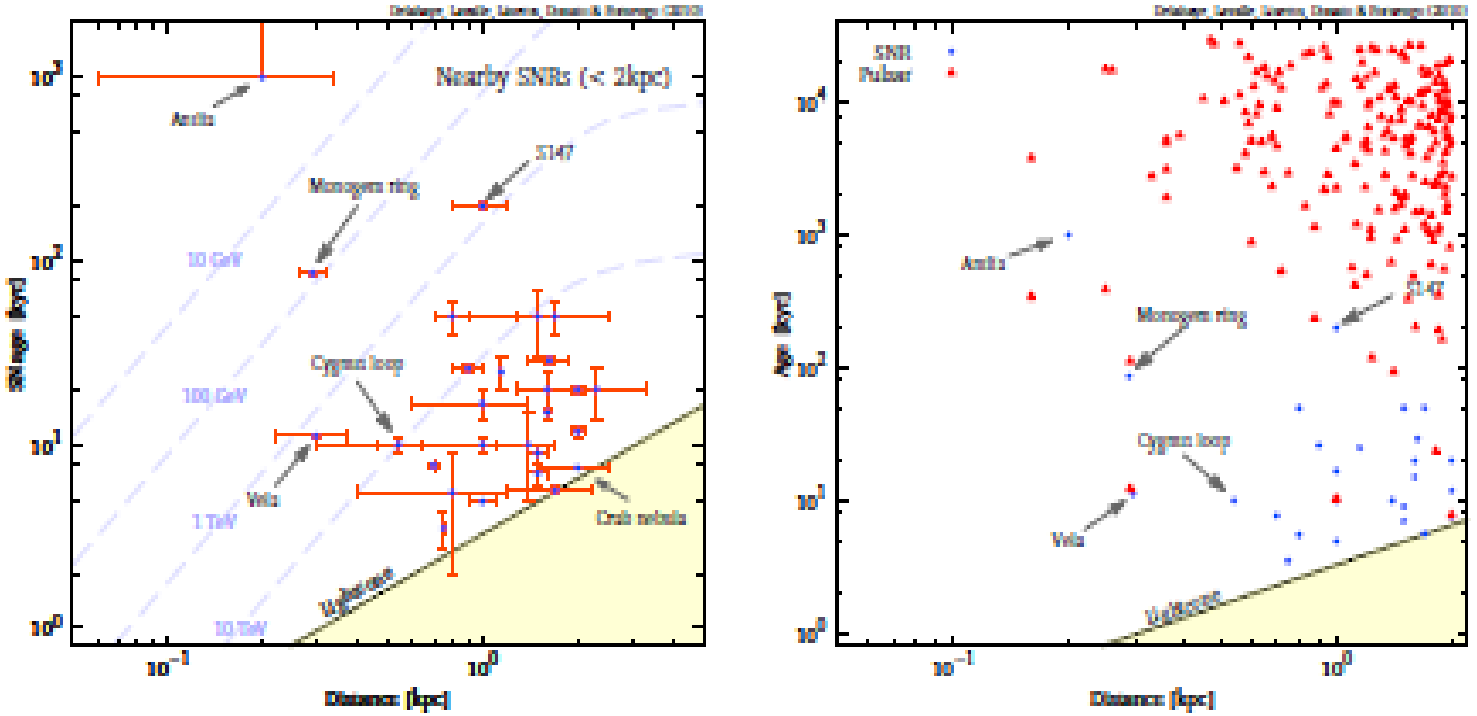

Fig. 9. Left: Plot of the *observed* age versus distance to the Earth for our sample of local SNRs (and associated uncertainties, see Table C.1). The dashed lines correspond to limits beneath which a local source cannot contribute significantly to the signal at the corresponding energy (valid only in the *med* propagation model — see Table 1). Indeed the age sets an upper limit, while the distance sets a lower limit to the energy range – see Sect. 4.4. Right: Same plot for our complete sample of local SNRs and pulsars.

Local 27-SNe

#	SNR G+long+lat	other name	distance [kpc]	radio index	Brightness [Jy]	age [kyr]	Pulsar
1	18.9-1.1		2. ± 0.1	0.28	40	11.75 ± 0.85	?
2	65.3+5.7		0.9 ± 0.1	0.58 ± 0.07	52	26 ± 1	-
3	65.7+1.2	DA 495	1.0 ± 0.4	0.45 ± 0.1	5	16.75 ± 3.25	unknown
4	69.0+2.7	CTB 80	2.0 ± 0.1	0.20 ± 0.10	60 ± 10	20 ± 1	J1952+3252
5	74.0-8.5	Cygnus Loop	$0.54^{+0.10}_{-0.08}$	0.4 ± 0.06	175 ± 30	10 ± 1	-
6	78.2+2.1	γ Cygni	1.5 ± 0.1	0.75 ± 0.03	275 ± 25	7 ± 1	-
7	82.2+5.3	W63	2.3 ± 1.0	0.36 ± 0.08	105 ± 10	20.1 ± 6.6	-
8	89.0+4.7	HB 21	1.7 ± 0.5	0.27 ± 0.07	200 ± 15	5.60 ± 0.28	-
9	93.7-0.2	CTB 104A or DA 551	1.5 ± 0.2	0.52 ± 0.12	42 ± 7	50 ± 20	-
10	114.3+0.3		0.7	0.49 ± 0.25	6.4 ± 1.4	7.7 ± 0.1	-
11	116.5+1.1		1.6	0.16 ± 0.11	10.9 ± 1.2	20 ± 5	B2334+61 ?
12	116.9+0.2	CTB 1	1.6	0.33 ± 0.13	6.4 ± 1.4	20 ± 5	B2334+61 ?
13	119.5+10.2	CTA 1	1.4 ± 0.3	0.57 ± 0.06	42.5 ± 2.5	10 ± 5	J0010+7309
14	127.1+0.5	R5	1.±0.1	0.43 ± 0.1	12 ± 1	25 ± 5	-
15	156.2+5.7		0.8 ± 0.5	$2.0^{+1.1}_{-0.7}$	4.2 ± 0.1	10 ± 1	B0450+55 ?
16	160.9+2.6	HB 9	0.8 ± 0.4	0.48 ± 0.03	∼ 75	5.5 ± 1.5	B0458+46
17	180.0-1.7	S147	1.2 ± 0.4	0.75	74 ± 12	600 ± 10	J0538+2817
18	184.6-5.8	Crab nebula or 3C144 or SN1054	2.0 ± 0.5	0.3	1,040	7.5 ⋆	B0531+31
19	189.1+3.0	IC 443	1.5 ± 0.1	0.36 ± 0.04	160 ± 5	30 or 4	-
20	203.0+12.0	Monogem ring	$0.288^{+0.033}_{-0.027}$			86 ± 1	B0656+14
21	205.5+0.5	Monoceros Nebula	1.63 ± 0.25	0.66 ± 0.2	156.1 ± 19.9	29 ± 1	-
22	263.9-3.3	Vela(XYZ)	0.295 ± 0.075	variable	2,000 ± 700	11.2 ± 0.1	B0833-45
23	266.2-1.2	RX J0852.0-4622 or Vela Jr or SN1300	0.75 ± 0.01			3.5 ± 0.8 ⋆?	J0855-4644 ?
24	276.5+19.0	Antlia	0.2 ± 0.14			≥ 1,000	B0950+08
25	315.1+2.7		1.7 ± 0.8	0.7		50 ± 10	J1423-56
26	330.0+15.0	Lupus Loop	1.2 ± 0.3			50 ± 10	B1507-44 ?
27	347.3-0.5	SN393	1.± 0.3			4.9 ⋆	-

Table C.1. Characteristics of nearby SNRs. Spectral index and brightness are inferred from measurements made at 1 GHz. Uncertainties in bold are not taken from bibliographic references, but just correspond to a rough uncertainty in the last relevant digit; hence they can be underestimated. An age is flagged with a ⋆ for an historical remnant; in this case, the age uncertainty is set from the distance uncertainty. Note that these ages are the *observed* ages, which differ from the *actual* ages by d/c.

Results without local catalog-01

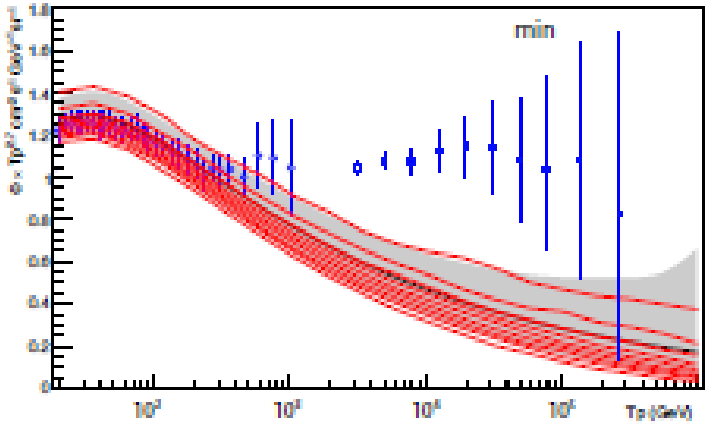

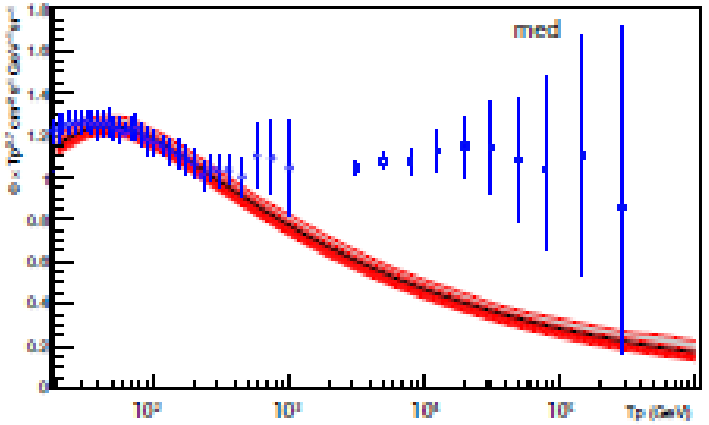

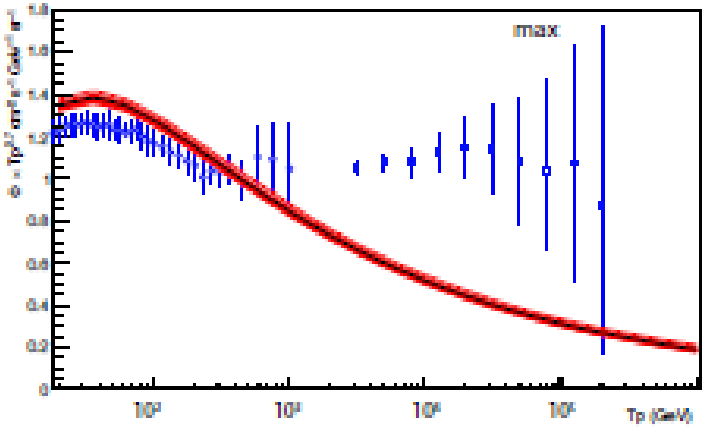

model	D_0 (kpc · My^{-1})	δ	L (kpc)	V_c (km · s^{-1})
min	0.0016	0.85	1	13.5
med	0.0112	0.7	4	12
max	0.0765	0.46	15	5

Results with local catalog-01

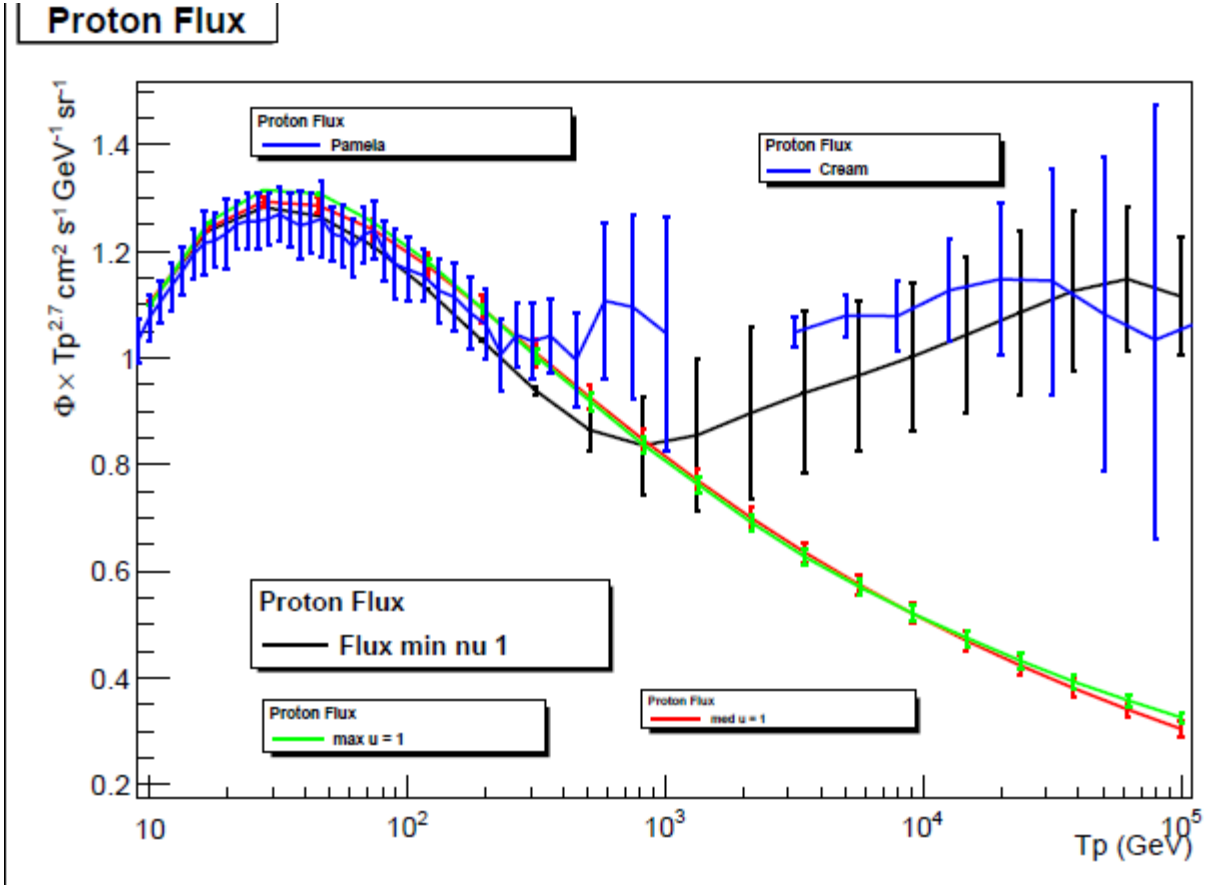

model	D_0 (kpc · My^{-1})	δ	L (kpc)	V_c (km · s^{-1})
min	0.0016	0.85	1	13.5
med	0.0112	0.7	4	12
max	0.0765	0.46	15	5

Scan of the parameter space:

- CR propagation is specified by K_0, δ, V_C and L
- The injection rate of CR species j is assumed as

$$q_j(p) = q_j^0 \left(\frac{p}{1\ GeV/nuc}\right)^{-\alpha_j}$$

  and to be the same for all CR sources.

- They are specified by the parameters $q_p^0,\ q_{He,}^0\ \alpha_p$ and α_{He}
- The average supernova explosion rate ν per 100 years.

- We have used these parameters to compute the proton and helium fluxes $\overline{\Phi}_{ext} + \Phi_{cat}$

DM halo profiles

From N-body numerical simulations:

$$\text{NFW}: \quad \rho_{\rm NFW}(r) = \rho_s \frac{r_s}{r}\left(1+\frac{r}{r_s}\right)^{-2}$$

$$\text{Einasto}: \quad \rho_{\rm Ein}(r) = \rho_s \exp\left\{-\frac{2}{\alpha}\left[\left(\frac{r}{r_s}\right)^{\alpha}-1\right]\right\}$$

$$\text{Isothermal}: \quad \rho_{\rm Iso}(r) = \frac{\rho_s}{1+(r/r_s)^2}$$

$$\text{Burkert}: \quad \rho_{\rm Bur}(r) = \frac{\rho_s}{(1+r/r_s)(1+(r/r_s)^2)}$$

$$\text{Moore}: \quad \rho_{\rm Moo}(r) = \rho_s \left(\frac{r_s}{r}\right)^{1.16}\left(1+\frac{r}{r_s}\right)^{-1.84}$$

At small r: $\rho(r) \propto 1/r^{\gamma}$

DM halo	α	r_s [kpc]	ρ_s [GeV/cm^3]
NFW	–	24.42	0.184
Einasto	0.17	28.44	0.033
EinastoB	0.11	35.24	0.021
Isothermal	–	4.38	1.387
Burkert	–	12.67	0.712
Moore	–	30.28	0.105

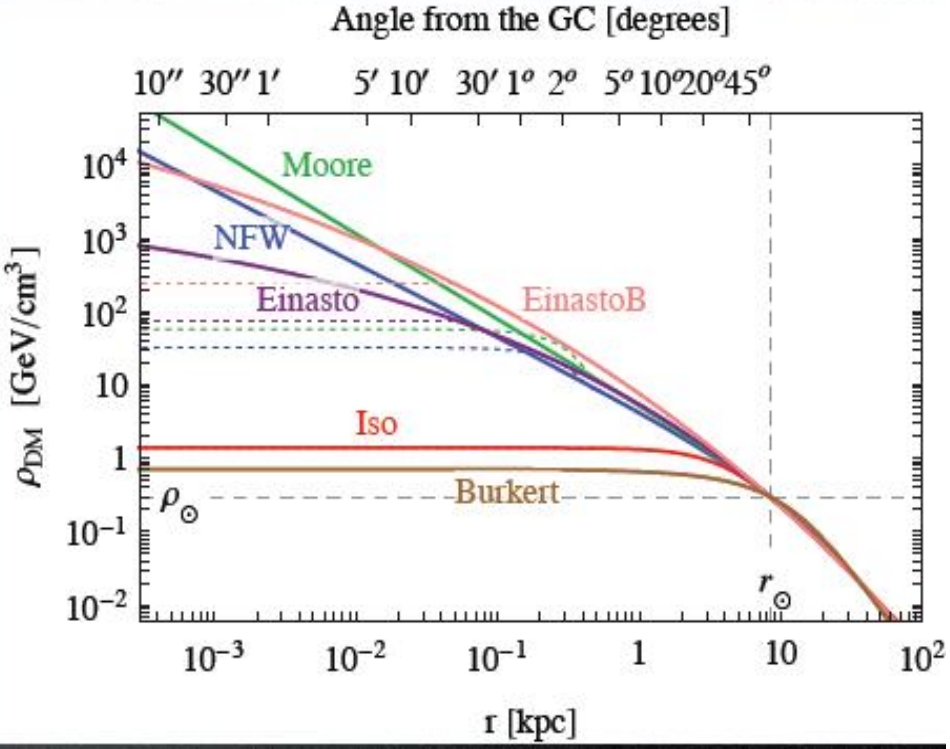

6 profiles:

- cuspy: NFW, Moore
- mild: Einasto
- smooth: isothermal, Burkert

EinastoB = steepened Einasto
(effect of baryons?)

Various Energy Loss Rates

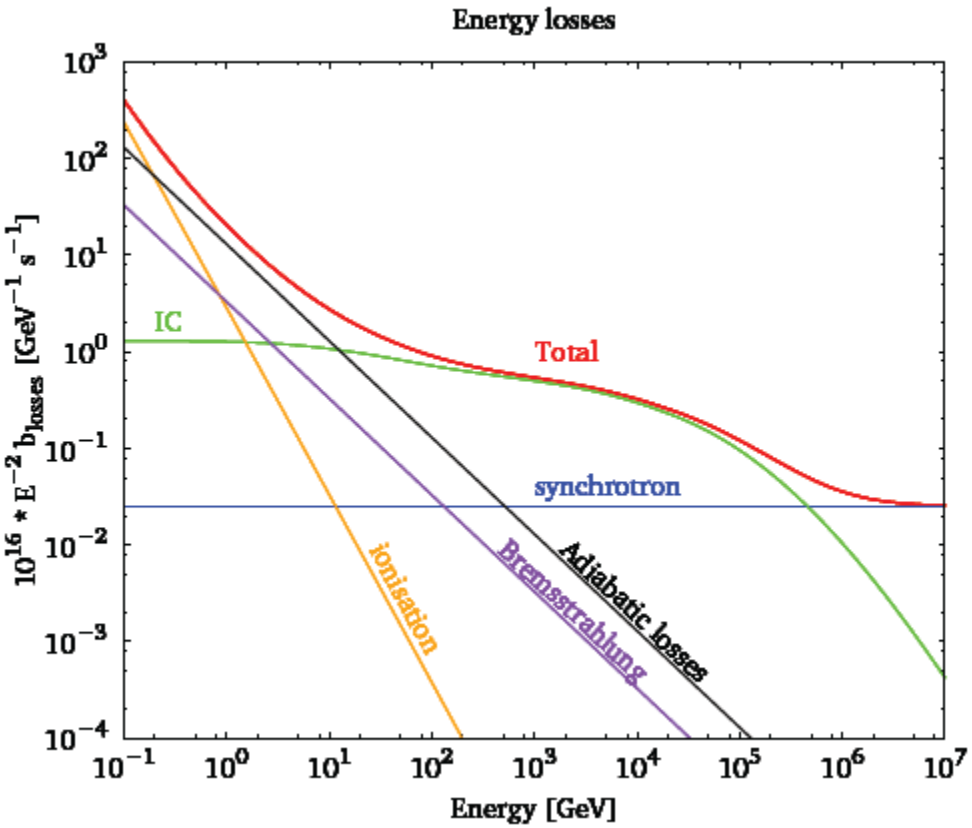

Spatial Distribution Models for Supernova remnants and pulsars

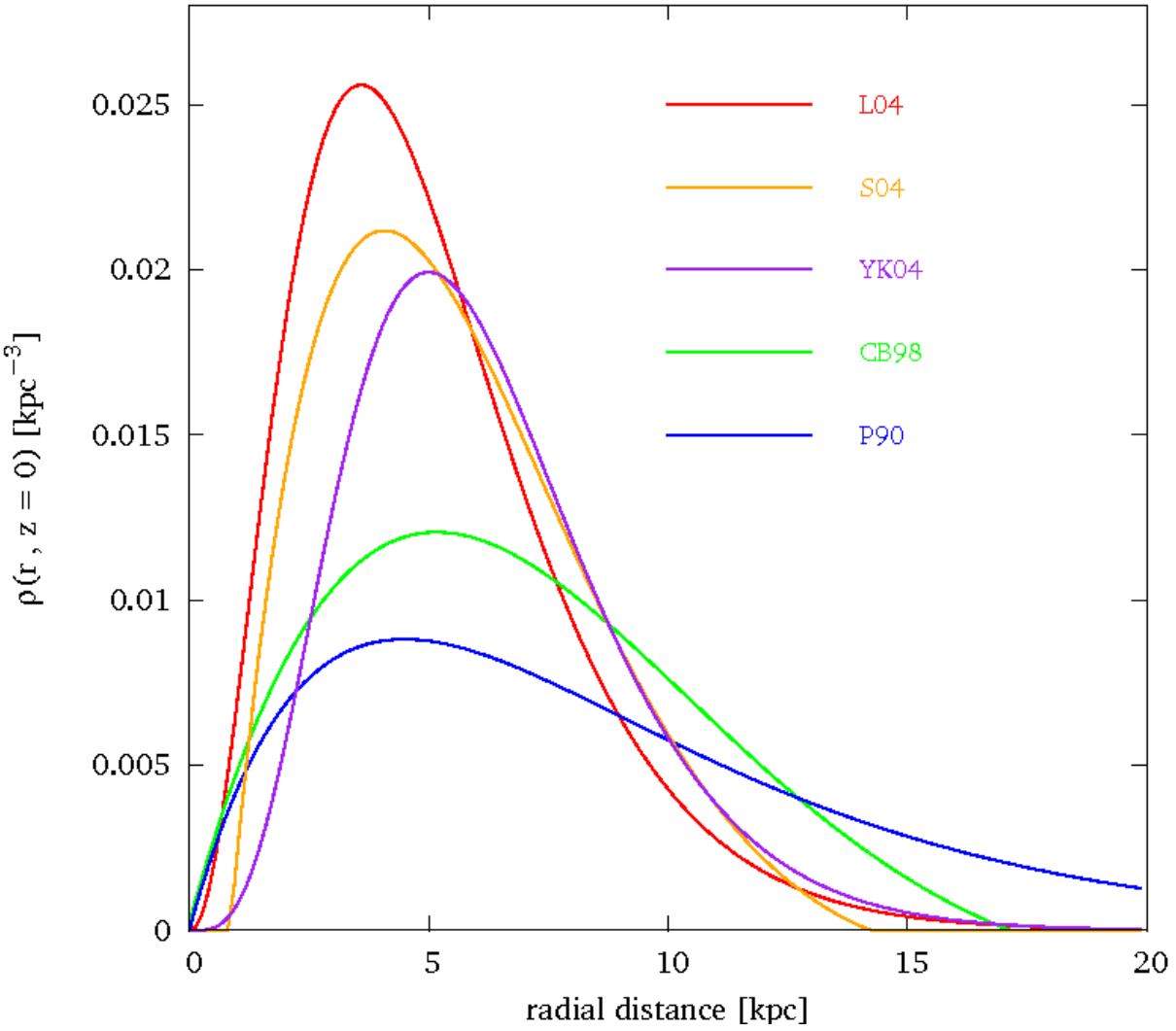

Results without local catalog-01

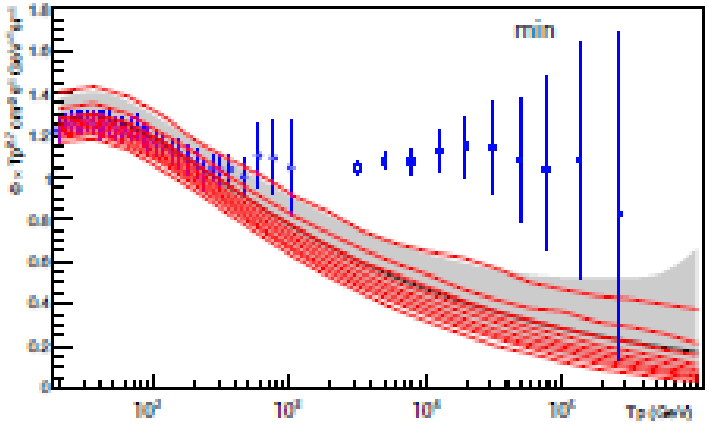

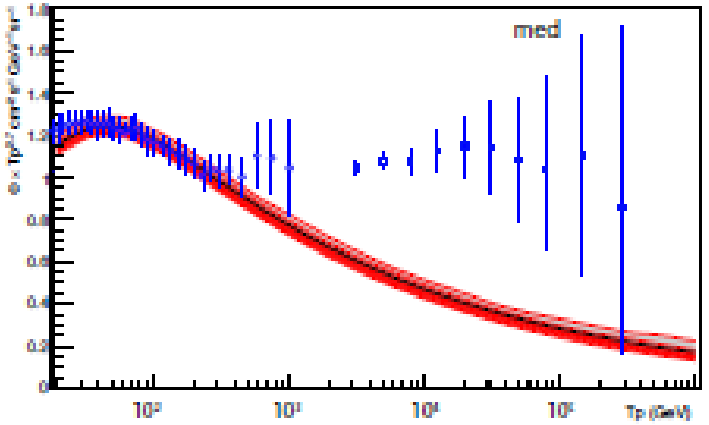

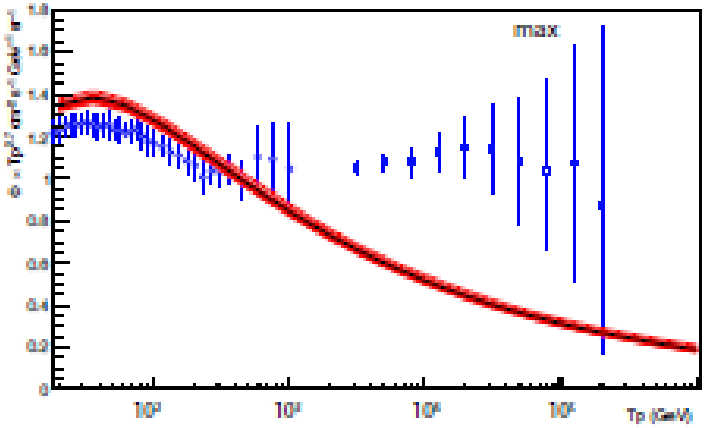

model	D_0 (kpc · My^{-1})	δ	L (kpc)	V_c (km · s^{-1})
min	0.0016	0.85	1	13.5
med	0.0112	0.7	4	12
max	0.0765	0.46	15	5

Results without local catalog-02

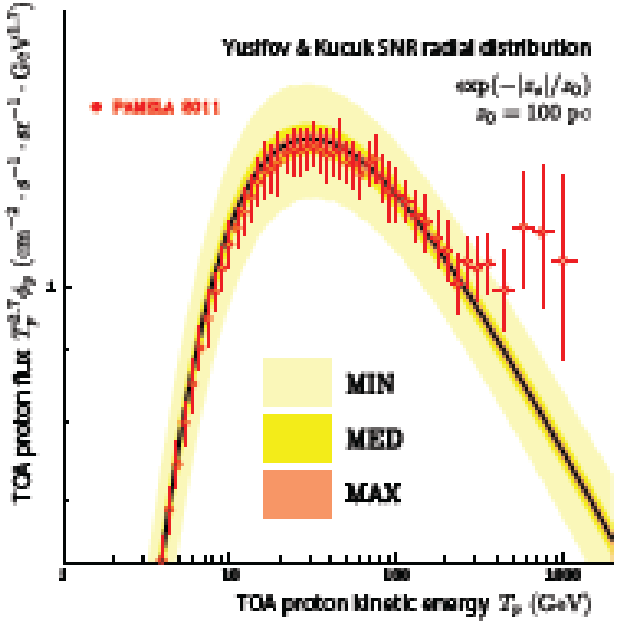

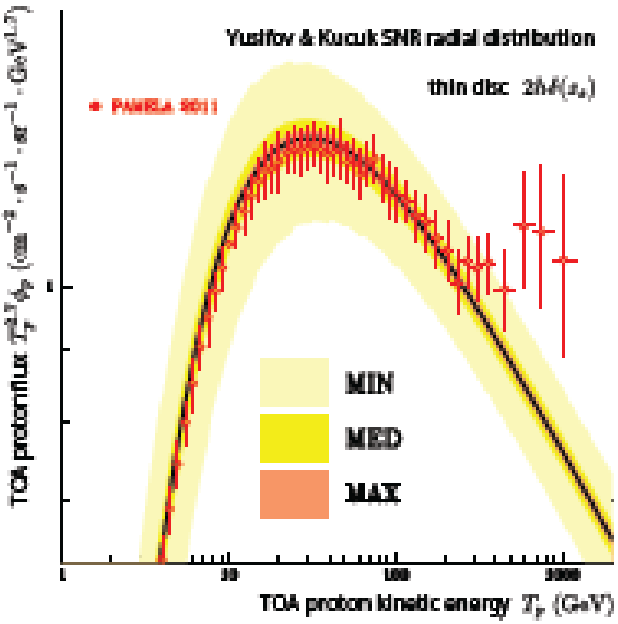

model	D_0 (kpc · My^{-1})	δ	L (kpc)	V_c (km · s^{-1})
min	0.0016	0.85	1	13.5
med	0.0112	0.7	4	12
max	0.0765	0.46	15	5

Results for Model B: same parameter sets with Model A, but nu=1.4 instead of 0.8/100 years

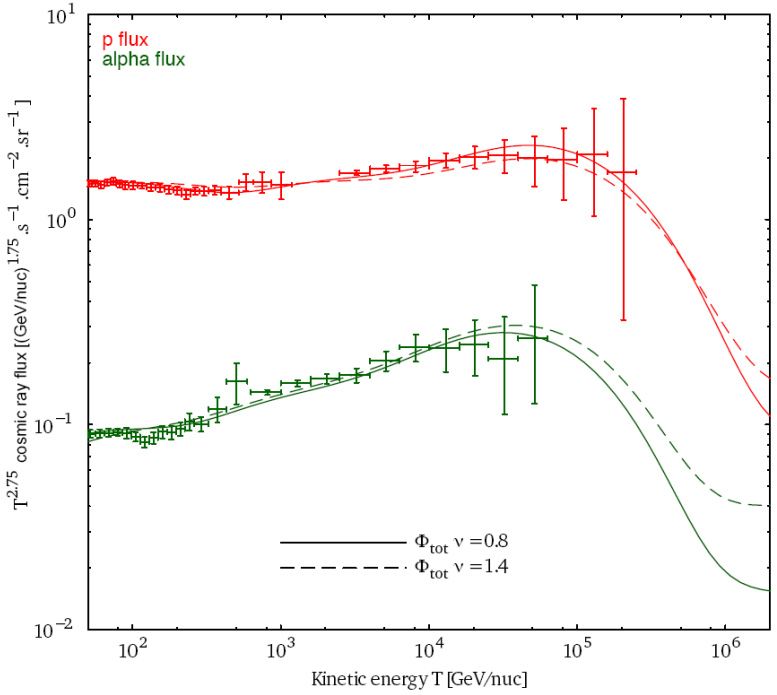

Fig. 2. Same as previous figures for models A and B (see Table 1), for two values of the supernovae explosion rate, $\nu = 0.8$ century^{-1} and $\nu = 1.4$ century^{-1}.

Results for Model C: MED parameter sets with best fits the B/C ratio, L=4 kpc

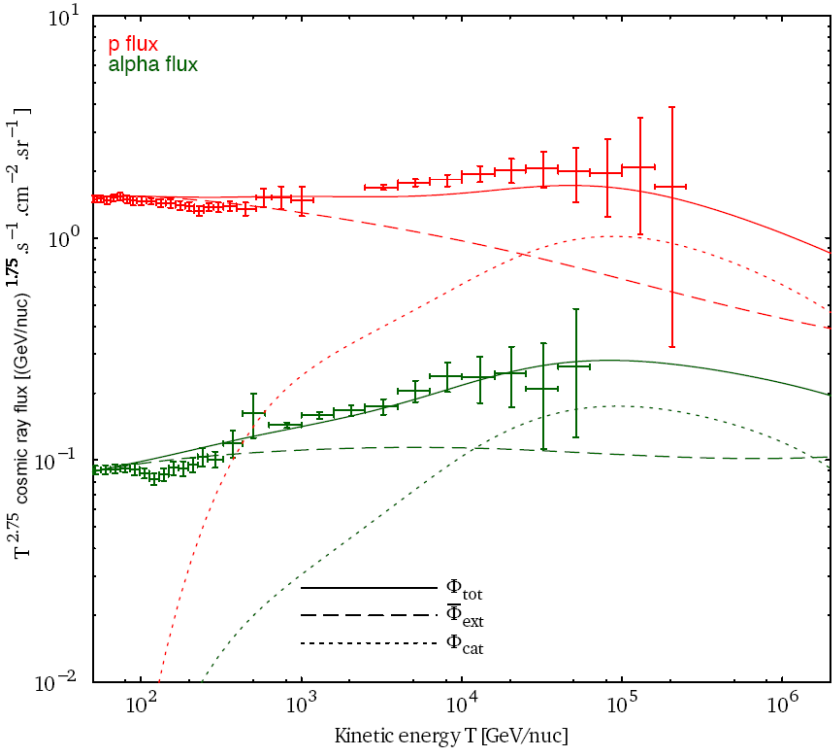

Fig. 3. Same as before, for the MED propagation parameters (see Table 1).

Secondary positron flux:

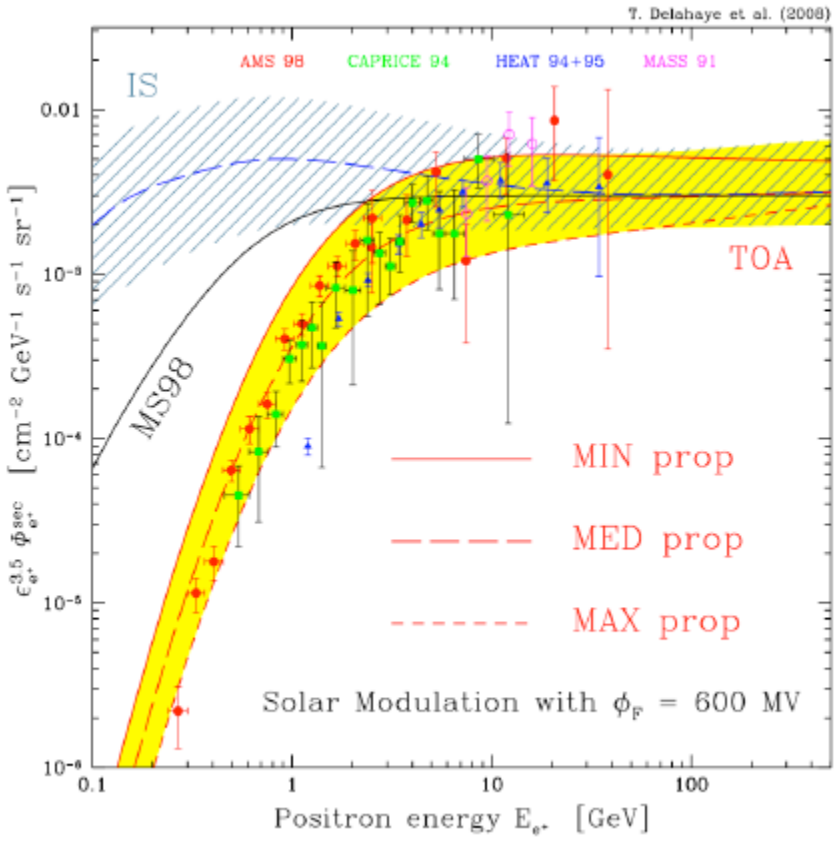

Positron-03: DM contributions

Donato et al., PRL 102, 071301 (2009)

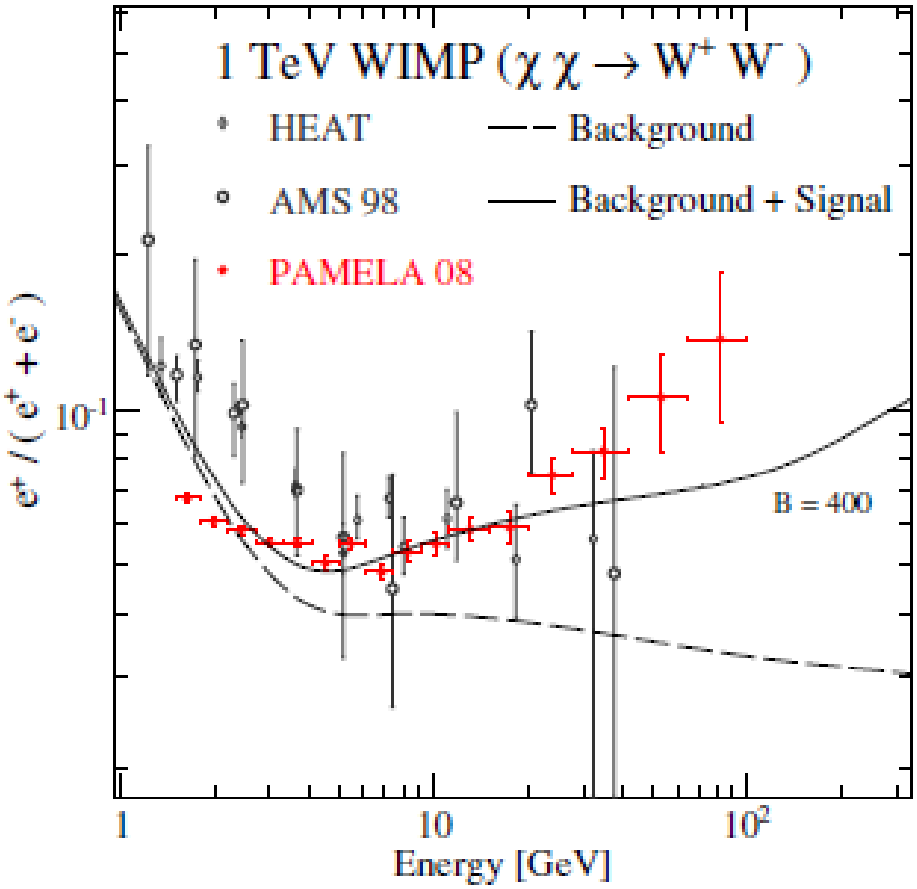

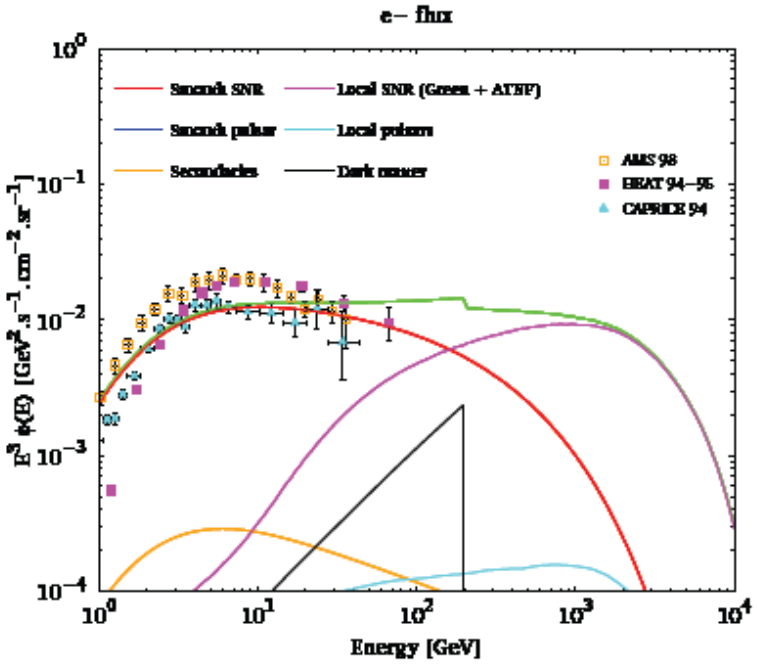
e− flux
Smooth SNR
Local SNR (Green + ATNF)
Smooth pulsar
Local pulsars
Secondaries
Dark matter
AMS 98
HEAT 94−95
CAPRICE 94
E³ φ(E) [GeV².s⁻¹.cm⁻².sr⁻¹]
Energy [GeV]

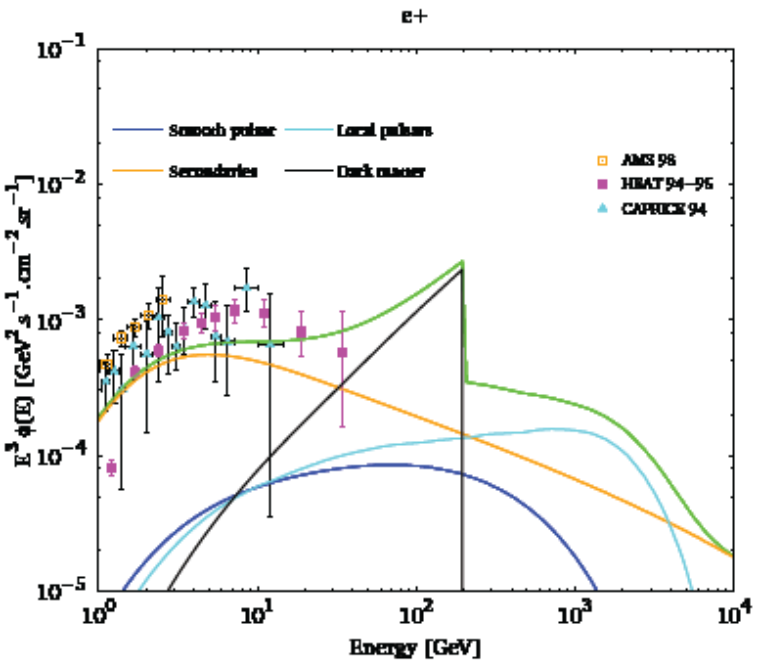
e+
Smooth pulsar
Local pulsars
Secondaries
Dark matter
AMS 98
HEAT 94−95
CAPRICE 94
E³ φ(E) [GeV².s⁻¹.cm⁻².sr⁻¹]
Energy [GeV]

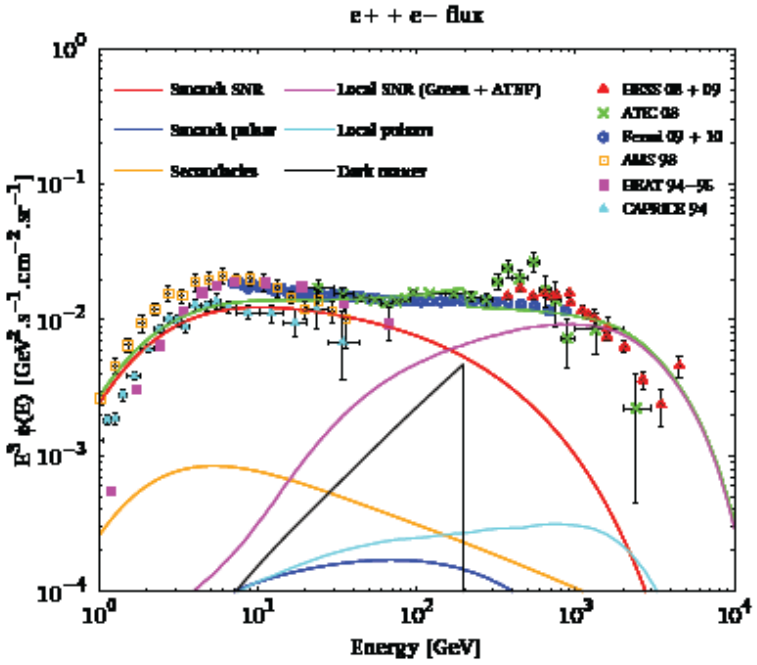
e+ + e− flux
Smooth SNR
Local SNR (Green + ATNF)
Smooth pulsar
Local pulsars
Secondaries
Dark matter
HESS 08 + 09
ATIC 08
Fermi 09 + 10
AMS 98
HEAT 94−95
CAPRICE 94
E³ φ(E) [GeV².s⁻¹.cm⁻².sr⁻¹]
Energy [GeV]

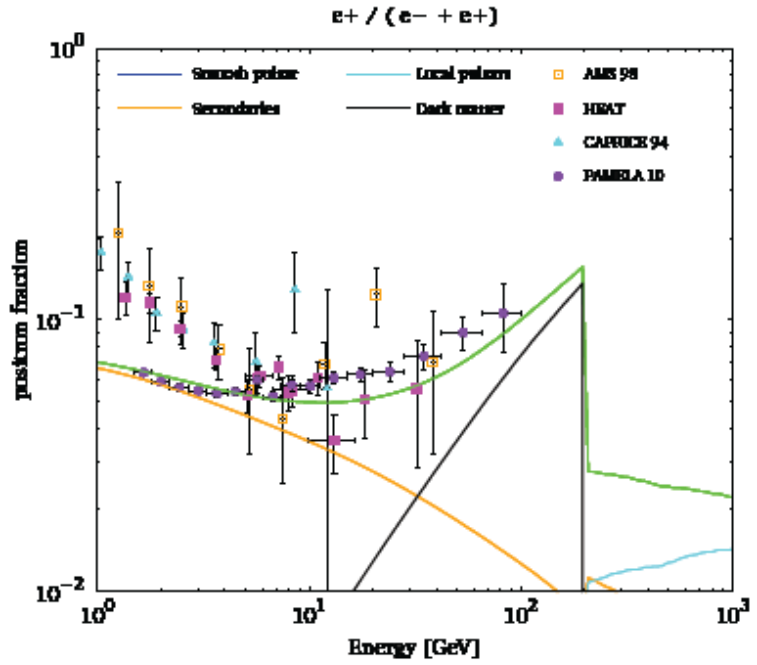
e+ / (e− + e+)
Smooth pulsar
Local pulsars
Secondaries
Dark matter
AMS 98
HEAT
CAPRICE 94
PAMELA 10
positron fraction
Energy [GeV]

Obsevation data and predictions (antiproton)

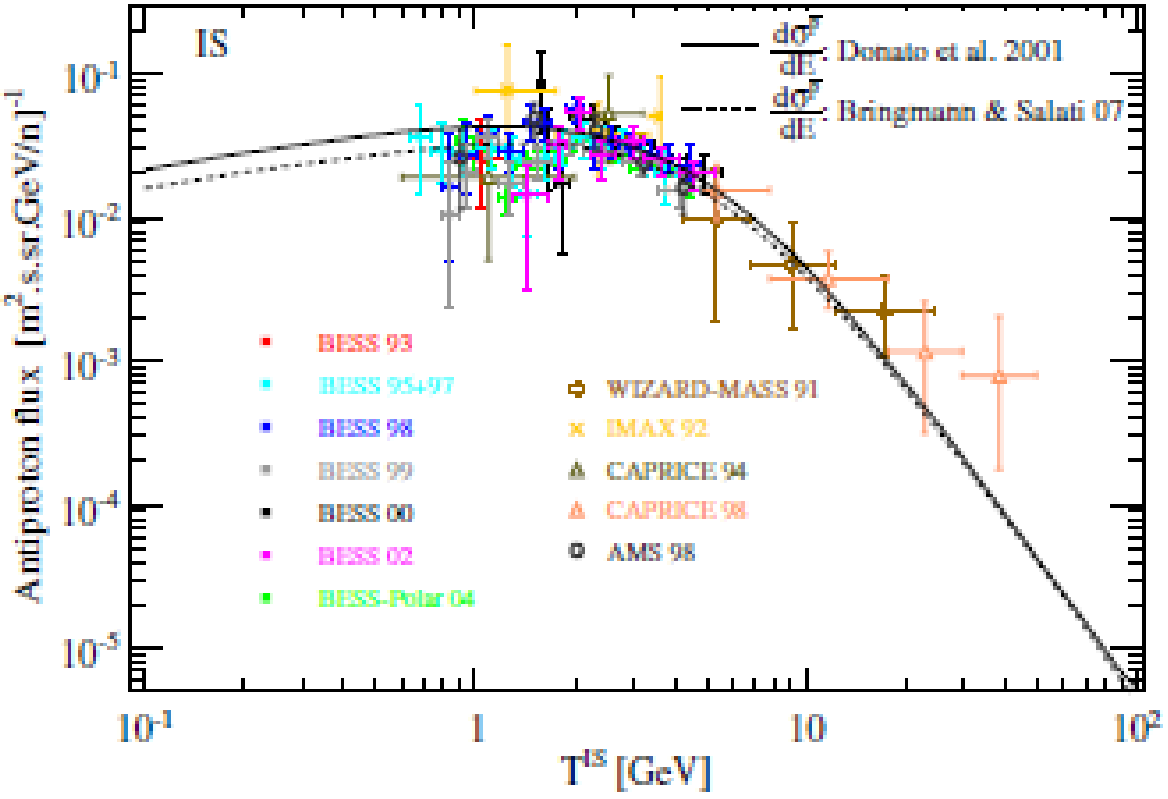

Antiproton-02:

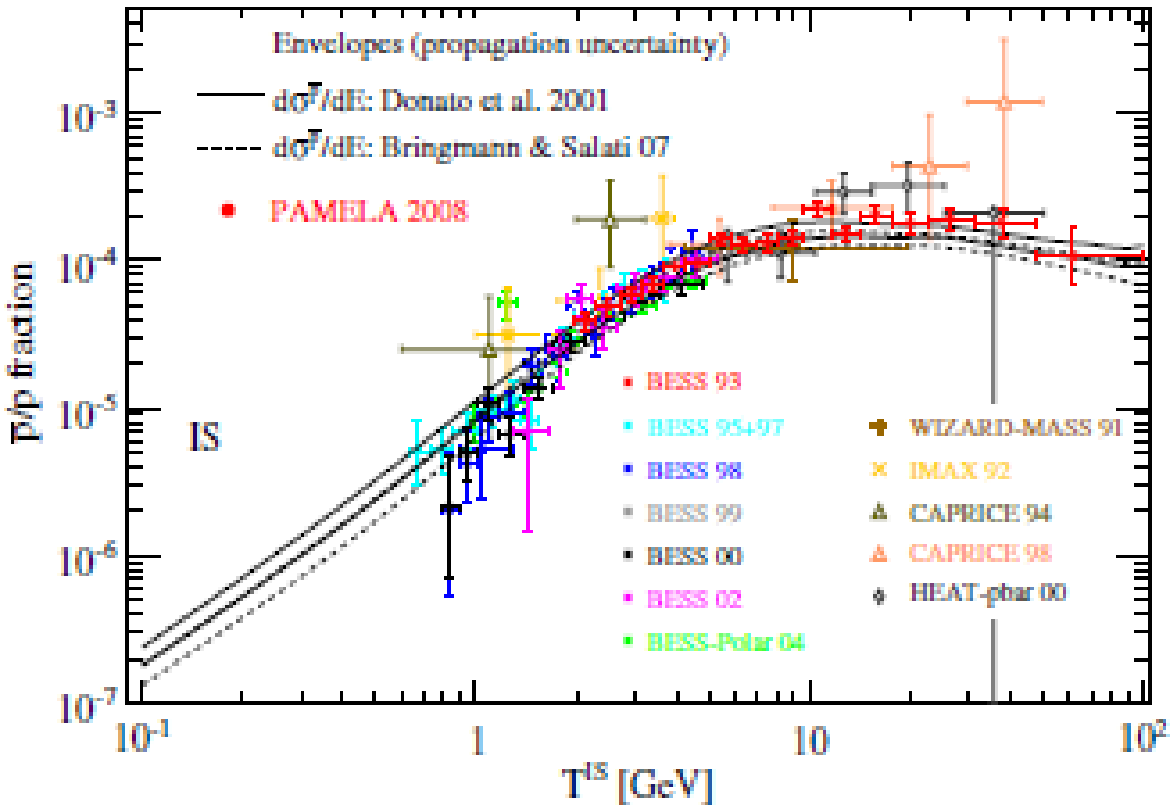

Antiproton-03: